

## PROSPECTS IN MESON SPECTROSCOPY\*

David W. G. S. Leith

Stanford Linear Accelerator Center, Stanford University, Stanford, Ca., 94305

### ABSTRACT

A review of the prospects for experimental meson spectroscopy is presented. The history of baryon spectroscopy is given and the lesson for meson studies is underlined. Several areas of new opportunity for meson experiments are described — namely, the new multiparticle spectrometers, their application to photoproduction investigations, and the new generation of  $e^+e^-$  colliding beam facilities. Accumulating evidence for the existence of meson towers is presented. Finally, the possible use of high energy and large momentum transfer to give a new (more democratic) look at the meson world, is discussed.

### INTRODUCTION

Before taking our "perspective" on the future of meson spectroscopy, I feel that it is important to say something to justify the very large efforts in new experiments and data analysis which are the natural extension of what we have heard these last two days, and which is also the strong conclusion of this review. I am also partly prompted to make these pious remarks as a defensive reaction to the title the organizing committee were originally bandying about — "Is there any point doing experiments below 50 GeV?"

I think the answer to that question is "yes", and that, at least for the moment, the study of meson spectroscopy is both important and fundamental. The goal of our high energy physics endeavours is to find the basic building blocks of matter, to explain the forces between them and the dynamics of their interactions. In our attempt to achieve these ends we make models which supposedly describe nature. In turn, these models have something to say about how the basic constituents of matter "dress" themselves for the observable world and of their properties. One of the important ways we have of learning more, is by confronting the predictions of these theories with data on the spectrum of particles which exist in nature, and on their specific properties. Therefore, the study of meson spectroscopy is not merely a botanical collecting of numbers, not just "stamp collecting", but it is, in fact, one of the main testing grounds of our understanding of fundamental processes.

One of the other conclusions of this meeting must be that there is a great deal still to do in the field of meson spectroscopy and that there are very many unanswered questions close to the heart of our understanding of the classification of resonant states.

In the following sections we will review the history of baryon spectroscopy and the lessons that it holds for meson spectroscopy, (Section II); look at the classification of the known meson states and what needs to be done to clarify the situation, and consider the new experimental opportunities becoming available — (the multiparticle spectrometers (MPS, OMEGA, LASS); the new possibilities for photoproduction studies; and the new generation of  $e^+e^-$  storage

---

\* Work supported by the U. S. Atomic Energy Commission.

(Invited talk presented at the IVth International Conference on Experimental Meson Spectroscopy, Northeastern University, Boston, Mass, April 26-27, 1974)

ring facilities) — Section III; gather the evidence for the existence of towers of meson states, (Section IV); briefly exort new efforts in search of exotic states (Section V); and finally present the possibility that high energy and large  $P_T$  collisions may be a useful tool to look at the meson world, (Section VI).

### BARYON HISTORY AND ITS LESSON FOR MESON SPECTROSCOPY

Baryon spectroscopy is in rather good shape and has, in recent years, been the major testing ground for our theoretical ideas on the classification of resonant states. The good progress in this field is in large proportion due to the intense and systematic programs of many groups over the last 10-15 years. An indicator of the quality of the data is given in Fig. 1. The total

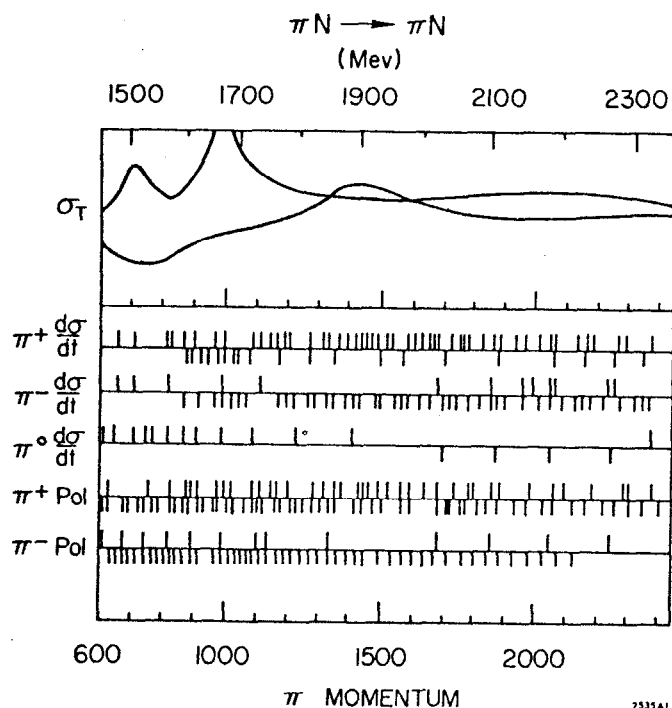


FIG. 1--Summary of data used in elastic phase shift analysis.

cross sections have been accurately measured every (5-10) MeV, and the  $\pi^\pm p$  elastic and charge exchange cross sections measured every (10-20) MeV up to 2500 MeV. Systematic polarisation measurements for  $\pi^\pm p$  elastic scattering complete the story. Detailed analysis of this data — the elastic phase shift analysis programs of Lovelace<sup>1</sup>, and Bareyre<sup>2</sup> — have provided most of the information on  $N^*$  resonances to date. It is interesting to note the scale of these analyses — the recent study of  $\pi N$  scattering by Lovelace<sup>2</sup> used some 25,000 data points. The situation for  $\Lambda$ 's and  $\Sigma$ 's is also in fair shape thanks to a comparably systematic study of the s-channel  $K^-p$  reactions,<sup>3</sup> ( $K^-p \rightarrow K^-p, \bar{K}^0n, \pi\Lambda, \Sigma\pi$ ).

To see the sensitivity of the partial wave analysis technique, let us examine the total cross sections for  $\pi^-p$  as shown in Fig. 2. One sees clear indications of the bump structure which was initially identified as the 1st, 2nd, 3rd  $\pi N$  resonances. However, below the cross sections, shown as arrows, are the various  $\pi N$  resonances found in the phase shift analysis described above. The number of resonant states far exceeds the visible structure in the cross section. These analyses are approaching their limit of sensitivity — resonances with couplings to the  $\pi N$  channel  $\times_{\pi N} \gtrsim 0.1$  are being found, but states with weaker coupling will have to be investigated in production experiments where they may be formed in a more favorable channel (e.g. via  $\rho$ -exchange).

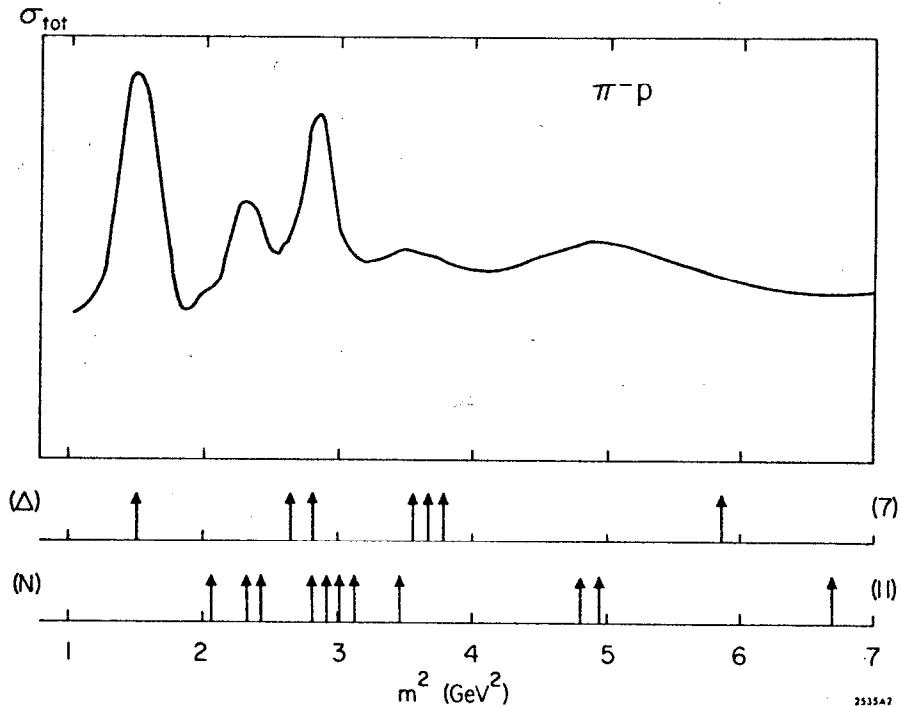


FIG. 2-- $\pi^-p$  total cross section structure and the resonances found in partial wave analyses.

We know a great deal about the resonances (mass, width,  $x_{\pi N}$ , J, P, I-spin) from these partial wave analyses, but we can never learn of the sign of the coupling constant (since that always appears squared in elastic processes),

$$\sigma(\pi N \rightarrow \pi N) \propto g_{\pi N}^2$$

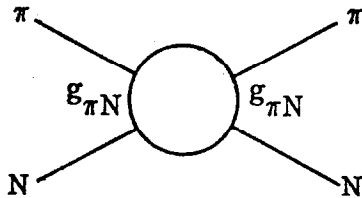


FIG. 3--Formation and decay of a resonance in elastic channel.

nor do we have any information on how the  $N^*$  states couple to other channels. As Gilman<sup>4</sup> has pointed out, it is just these parameters — the coupling signs and the branching ratio into the various decay modes — which we need to know for the classification of these states into the various supermultiplets.

To investigate these parameters one must study inelastic scattering. Some attempts at study of inelastic  $\pi N$  scattering have been undertaken in which the Dalitz Plot moments have been analysed, or cuts on the data have been made to isolate a quasi-two body reaction, (e.g.  $\pi N \rightarrow \Delta\pi$ ).<sup>5</sup> These studies were interesting and gave useful information on the dominant resonance structure, but were unable to make fullest use of the information inherent in the data. (Such treatment loses information on the interference between

states of different J, or different P, or different magnetic substate  $J_z$  — such interferences are very sensitive probes of the resonant structure within multibody reactions).

Recently a SLAC-LBL collaboration<sup>6,7</sup> has studied inelastic  $\pi N$  scattering in the reaction  $\pi N \rightarrow \pi\pi N$  at energies up to 2000 MeV using the isobar model.<sup>8</sup> There, the presence of overlapping resonances in the final state is taken into account, and an attempt is made to make use of the information contained in the interferences between the specific amplitudes. The transition amplitude for reaching a given final state is written as the coherent sum of the two body processes

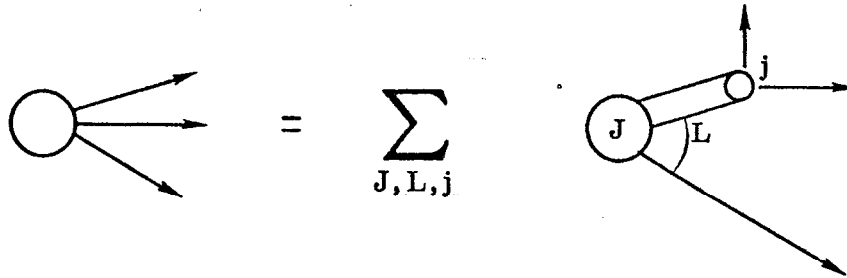


FIG. 4--Schematic description of the isobar model.

The amplitude is written

$$T(W, \omega_1, \omega_2, \alpha, \beta, \gamma)$$

$$= \sum_{J, L, S, I, l} A^{IJLSl}(W) C^I X^{JLSl}(W, \omega_1, \omega_2, \alpha, \beta, \gamma) B^L(\omega_1, \omega_2)$$

$\omega_1, \omega_2$  — energies,  $\alpha, \beta, \gamma$  — Euler angles

$C^I$  — C. G. coefficient products

$X$  — ang. mom. decomposition factor

$B$  — final state factor — (B.W. or Watson Theorem)

$A$  — the partial wave amplitudes.

The data on all single pion production processes were then fit at each center of mass energy, to determine the partial wave amplitudes,  $A^{IJLSl}$ . For  $\pi N \rightarrow \pi\pi N$ , we have three possible two-body final states:  $\Delta\pi$ ,  $\rho N$ ,  $\epsilon N$ .

Figure 5 shows the cross section for one of the single pion production reactions,  $\pi^- p \rightarrow \pi^+ \pi^- n$ , from (1300-2000) MeV. Below, an indication is given of the resonances found in each angular momentum wave from the partial wave analysis (PWA). Clearly, the PWA has been able to dig out much more structure than we could see in the cross section.

This analysis of the inelastic scattering allows an almost complete description of  $\pi N$  scattering up through 2000 MeV. In Table I the  $N^*$  resonances found in this energy region are listed, together with their various decay modes.

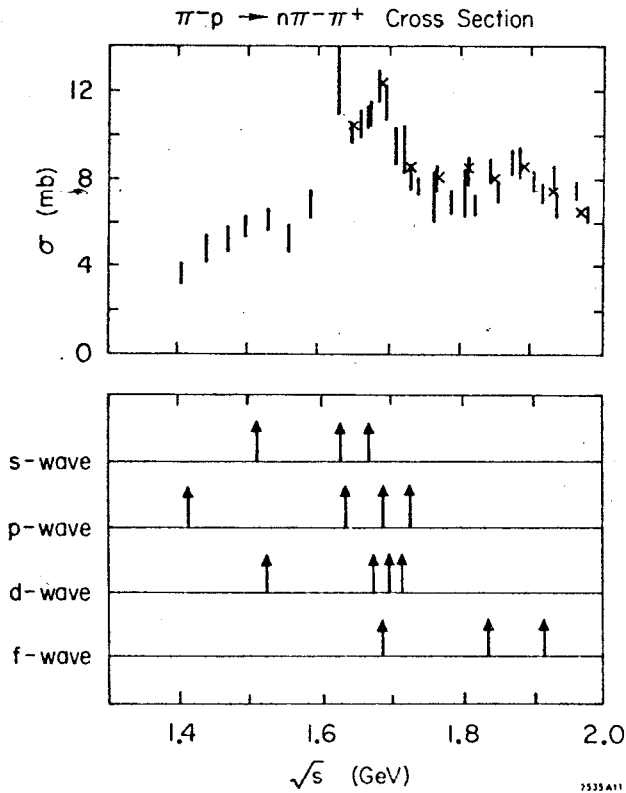


FIG. 5--The cross section for the reaction  $\pi^- p \rightarrow n \pi^- \pi^+$  in below 2000 MeV, and the resonant structure found from a partial wave analysis.

structure. The coupling strength to each decay mode is given by the amplitude of the circular motion, while the sign of the coupling is given by whether the amplitude points up (positive) or down (negative) on the Argand plot, at the resonant energy.<sup>10</sup>

Gilman,<sup>4</sup> and others,<sup>11</sup> have emphasized that coupling signs and branching ratios are very important for the classification of resonant states. Since the nucleon and the delta, (and the rho-meson and the pion) belong to the same SU(6) super-multiplet, the reactions

$$\pi N \rightarrow \pi N, \quad \pi N \rightarrow \pi \Delta$$

and

$$\pi N \rightarrow \pi N, \quad \pi N \rightarrow \rho N$$

are related by SU(6) Clebsch-Gordan coefficients. This allows the intermediate isobar state to be well characterized by its decay properties; this method was very successfully applied to the classification of several new states found in the  $\pi N$  isobar analysis.<sup>7,12</sup>

In summary, the lesson from baryon spectroscopy is that high statistics, systematic experiments together with sophisticated partial wave analysis

The final column shows the sum of all the measured branching ratios; it is interesting to observe that almost all the resonance coupling has been accounted for in this analysis.<sup>7</sup>

The inelastic partial wave analysis of the  $\pi N \rightarrow \pi \pi N$  reaction also provides an Argand diagram for each wave. The results for one wave, the P11 wave,<sup>9</sup> are reproduced in Fig.6. The Argand diagrams for the reactions  $\pi N \rightarrow \pi N, \pi \Delta, \rho N$  and  $\epsilon N$  are each displayed on the left, while on the right-hand side the energy dependence of the total inelastic cross section, and the square of the scattering amplitude for each of the inelastic reactions is plotted. Two resonances are found in this wave at 1415 MeV and 1730 MeV,<sup>6</sup> and from inspection of the energy dependence of the scattering amplitude one can see that the lower mass state couples to  $\Delta \pi$  and  $\epsilon N$ , while the 1730 MeV state couples to  $\Delta \pi, \rho N$  and  $\epsilon N$ . On the Argand plots on the left, one can see the circular anti-clockwise motion of the amplitude, characteristic of resonant

Table I N\* Couplings for LBL-SLAC Isobar Analysis.

Resonance	Mass	$\pi N$	$\pi \Delta$	$\rho N$	$\epsilon N$	$\Sigma x_i$
S <sub>11</sub>	1520	✓		✓	✓	0.4
S <sub>11</sub>	1675	✓	✓	✓	✓	0.8
S <sub>31</sub>	1625	✓	✓	✓		1.0
P <sub>11</sub>	1415	✓	✓		✓	1.0
P <sub>11</sub>	1730	✓	✓	✓	✓	1.0
P <sub>13</sub>	1695	✓		✓		1.0
P <sub>33</sub>	1900	✓	✓			1.0
D <sub>13</sub>	1525	✓	✓	✓		1.0
D <sub>13</sub>	1710	✓	✓	✓	✓	1.0
D <sub>33</sub>	1725	✓	✓	✓		1.0
D <sub>15</sub>	1660	✓	✓			1.0
F <sub>15</sub>	1680	✓	✓	✓	✓	1.0
F <sub>35</sub>	1870	✓	✓	✓		1.0
F <sub>37</sub>	1930	✓	✓	✓		0.8

studies (and not just bump hunting) are necessary for a complete probe of the full resonant structure. These studies must include both the elastic and the inelastic scattering channels; the former is probably the most sensitive probe of resonant structure (providing the coupling is large enough), but the latter is required for information on coupling signs and branching ratios, which are important in the classification of the states.

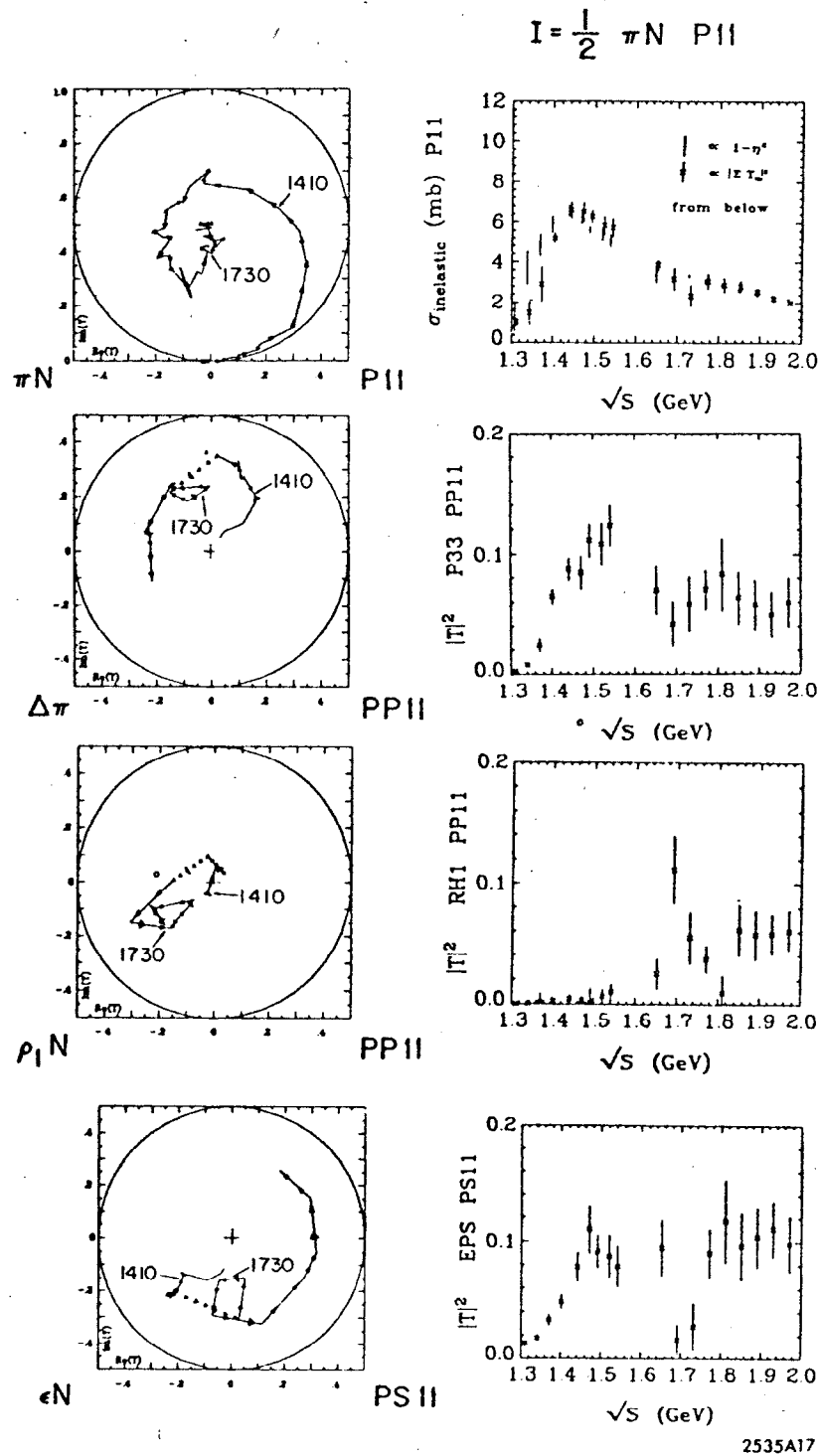


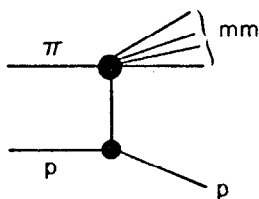
FIG. 6--The Argand plots and the energy dependence of the inelastic cross section and the scattering amplitudes for the  $\pi\Delta$ ,  $\rho N$  and  $\epsilon N$  sub-states, all for the P11 wave. These results are taken from the analysis of Ref. (6).

## MESON SPECTROSCOPY

### A. General.

The mesons are in a much sadder situation — or as Fox described it so poetically — "The Great Meson Scandal". The reasons for the discrepancy between the mesons and baryons are clear and well known — mesons may only be observed in production reactions, and therefore must couple strongly to a healthy exchange trajectory; form factors complicate production as a function of momentum transfer; the meson cloud round the proton (or the t-channel couplings) provide a very "low luminosity" target for meson experiments; — and we could go on.

An example of the complication in the meson world is found in considering the equivalent of the total cross section data discussed above. Figure 7 shows the missing mass spectrum in  $\pi^-p$  collision at 11 GeV/c, where the recoil proton was detected.<sup>13</sup>



This may be considered as a "total cross section" in a meson-meson collision. However, it is really the sum of many total cross sections, with each term having its own s- and t-dependence:

$$" \sigma " = a (s, t) \cdot \sigma (\pi P)$$

$$+ b (s, t) \cdot \sigma (\pi \pi)$$

$$+ c (s, t) \cdot \sigma (\pi \rho)$$

$$+ \dots$$

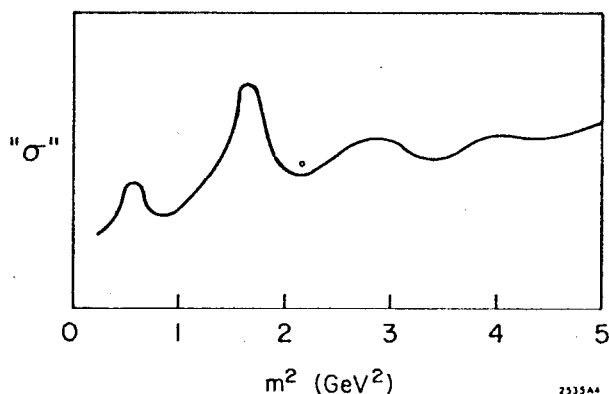


FIG. 7--The missing mass spectrum in the reaction  $\pi^-p \rightarrow p(MM)$ , which may be interpreted as a "total cross section" in a meson-meson scattering problem.

Fortunately, the lesson from baryon spectroscopy is that a detailed study of this structure is not very useful, and that we must settle down to the long, systematic programs of study of exclusive two-body and multibody scattering.

One area in which meson studies have some advantage over the corresponding baryon experiments is that the selection rules governing particle decays are much more stringent. For example, the  $\pi N$  channel couples to all  $I, J^P$  isobar states, while statistics,  $J^P, C, G, I$  — all combine to limit the various meson couplings. Table II<sup>14</sup> displays the effect of the selection rules for a few meson channels, to illustrate the point, for each of the  $J^P$  states in the  $L = 1$  and  $L = 2$  quark model supermultiplets. We notice that some decay modes,  $(\pi\rho, \pi\omega)$ , are quite selective while others, like  $K^*\bar{K}$  or  $K^*\bar{K}^*$ , couple to most spin-parity states. These properties may be very useful in different circumstances; for example, we might use one of the very selective channels to attempt to identify a very rare state, or use a decay mode like  $\bar{K}K^*$  when

measuring relative coupling signs through interferences of many overlapping resonances.

Table II Selection Rules for Meson Decays

DECAYS	0 <sup>++</sup>		1 <sup>++</sup>		1 <sup>+−</sup>		1 <sup>−−</sup>		2 <sup>++</sup>		2 <sup>−−</sup>		2 <sup>−+</sup>		3 <sup>−−</sup>	
	I=0	I=1														
$\pi\pi$	✓							✓	✓							✓
$K\bar{K}$	✓	✓					✓	✓	✓	✓					✓	✓
$\pi\omega$						✓		✓				✓				✓
$\eta\omega$					✓		✓				✓				✓	
$\pi\rho$				✓	✓		✓			✓	✓			✓	✓	
$K\bar{K}^*$			✓	✓	✓	✓	✓	✓	✓	✓	✓	✓	✓	✓	✓	✓
$K^*\bar{K}^*$	✓	✓	✓	✓	✓	✓	✓	✓	✓	✓	✓	✓	✓	✓	✓	✓

The emphasis for meson spectroscopy is then to concentrate on amplitude structure in elastic and inelastic exclusive processes. Some substantial progress has been made already:

- the  $\pi$ - $\pi$  scattering studies, especially the beautiful experiment and analysis of the CERN Munich Group, described by Manner<sup>15</sup> at this conference;
- the K- $\pi$  scattering analyses from LBL,<sup>16</sup> CERN<sup>17</sup> and now in progress at SLAC.<sup>18</sup>

These analyses have brought out the dominant elastic meson-meson structure very clearly, and the continuing work on the  $\pi$ - $\pi$  data<sup>15</sup> is now beginning to see exciting signs of underlying structure below the  $\rho$ ,  $f$  and  $g$  mesons.

- the inelastic scattering analysis package of Ascoli,<sup>19</sup> which has been successfully used in several studies of  $\pi \rightarrow 3\pi$  and  $K \rightarrow K\pi\pi$ ;
- the development of the LBL-SLAC s-channel isobar model program to deal with production reactions, reported by Lasinski<sup>20</sup> at this meeting, and being applied to  $\pi \rightarrow 3\pi$  studies at LBL,<sup>21</sup> and to  $K \rightarrow K\pi\pi$  at SLAC.<sup>22</sup>

It is good to have these two independent partial wave analysis programs based on different assumptions and using quite different fitting methods. Ascoli's package fits the density matrix elements,  $\rho_{ij}$ , while the program described by Lasinski attempts to fit the scattering amplitudes.

- new insights on these analyses of inelastic scattering in production reactions should come from the analysis of a Cal-Tech— LBL-SLAC<sup>23</sup> experiment studying;

$$\pi^{\pm} p \rightarrow \pi_f^{\pm} (p\pi^+ \pi^-) \quad \text{at 14 GeV/c}$$

using a hybrid spark chamber — bubble chamber set-up. A comparison of the  $N\pi\pi$  amplitudes from this experiment with those obtained in the

s-channel SLAC-LBL experiment<sup>6,7</sup> described above, should bring to light any unusual, unexpected t-channel effects for these production amplitude analyses. (See Fig. 8.)

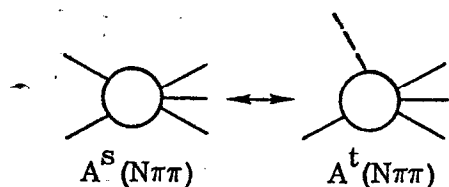


FIG. 8--The comparison of the amplitude for  $N^* \rightarrow N\pi\pi$  derived from s-channel studies (see Refs. 6, 7) and from t-channel studies (see Ref. 23).

### B. Classification.

The talk by Gilman<sup>4</sup> discussed the quark model and some aspects of classification. Let me quickly recap the rules of the model:

- quarks belong to the  $\underline{3}$  group of SU(3), and are the elementary units of all SU(3) representations;
- mesons are made up of qq pairs, which implies that they will be found in the  $\underline{8}$ , and  $\underline{1}$  SU(3) representations and only in those groups;
- the quarks have spin 1/2, which implies that mesons will have integral spin;
- the qq system undergoes orbital excitation, such that the parity of a system,  $P = (-1)^{L+1}$  and the total angular momentum,  $J = \underline{L} + \underline{S}$ .

Thus, within the quark model, we expect supermultiplets with  $L=0,1,2$ , - where L is the orbital angular momentum in the qq system. The resulting multiplet structure is summarized in Fig. 9, where we have also tried to assign known meson states to the various  $J^{PC}$  multiplets. The table also gives an indication of whether the  $I=0$  members of the various multiplets might be expected to be unmixed (like the  $\eta, \eta'$ ), magically mixed (like the  $\omega, \phi$ ) or complicated ( $\epsilon, S^*$  situation). The magically mixed are marked (●) on the right hand side. Remember, magically mixed means that the " $\phi$ -like meson" has only strange quarks and the " $\omega$ -like meson" has no strange quarks, i. e.

$$"\phi" \sim \lambda\bar{\lambda}$$

$$"\omega" \sim \frac{p\bar{p} + n\bar{n}}{\sqrt{2}}$$

FIG. 9--The  $L=0,1,2$  supermultiplets of the quark model.

$L=0$	{	$0^{-+}, 1^{--}$	
$L=1$	{	$0^{++}, 1^{++}, 1^{+-}, 2^{++}$	
$L=2$	{	$1^{--}, 2^{--}, 2^{-+}, 3^{--}$	

$L=0$	{	<table style="border-collapse: collapse; width: 100%; text-align: center;"> <tr> <td style="padding: 2px 10px;"><math>0^{-+}</math></td> <td style="padding: 2px 10px;"><math>\pi</math></td> <td style="padding: 2px 10px;"><math>\eta</math></td> <td style="padding: 2px 10px;"><math>\eta'</math></td> <td style="padding: 2px 10px;">K</td> </tr> <tr> <td style="padding: 2px 10px;"><math>1^{--}</math></td> <td style="padding: 2px 10px;"><math>\rho</math></td> <td style="padding: 2px 10px;"><math>\omega</math></td> <td style="padding: 2px 10px;"><math>\phi</math></td> <td style="padding: 2px 10px;"><math>K^*</math></td> </tr> </table>	$0^{-+}$	$\pi$	$\eta$	$\eta'$	K	$1^{--}$	$\rho$	$\omega$	$\phi$	$K^*$	(●)										
$0^{-+}$	$\pi$	$\eta$	$\eta'$	K																			
$1^{--}$	$\rho$	$\omega$	$\phi$	$K^*$																			
$L=1$	{	<table style="border-collapse: collapse; width: 100%; text-align: center;"> <tr> <td style="padding: 2px 10px;"><math>0^{++}</math></td> <td style="padding: 2px 10px;"><math>\delta</math></td> <td style="padding: 2px 10px;"><math>\epsilon</math></td> <td style="padding: 2px 10px;"><math>S^*</math></td> <td style="padding: 2px 10px;"><math>\kappa</math></td> </tr> <tr> <td style="padding: 2px 10px;"><math>1^{++}</math></td> <td style="padding: 2px 10px;"><math>A_1</math></td> <td style="padding: 2px 10px;">D</td> <td style="padding: 2px 10px;">?</td> <td style="padding: 2px 10px;"><math>Q^A</math></td> </tr> <tr> <td style="padding: 2px 10px;"><math>1^{+-}</math></td> <td style="padding: 2px 10px;">B</td> <td style="padding: 2px 10px;"><math>h^\omega</math></td> <td style="padding: 2px 10px;"><math>h^\phi</math></td> <td style="padding: 2px 10px;"><math>Q^B</math></td> </tr> <tr> <td style="padding: 2px 10px;"><math>2^{++}</math></td> <td style="padding: 2px 10px;"><math>A_2</math></td> <td style="padding: 2px 10px;">f</td> <td style="padding: 2px 10px;"><math>f'</math></td> <td style="padding: 2px 10px;"><math>K^{*1}</math></td> </tr> </table>	$0^{++}$	$\delta$	$\epsilon$	$S^*$	$\kappa$	$1^{++}$	$A_1$	D	?	$Q^A$	$1^{+-}$	B	$h^\omega$	$h^\phi$	$Q^B$	$2^{++}$	$A_2$	f	$f'$	$K^{*1}$	(●)
$0^{++}$	$\delta$	$\epsilon$	$S^*$	$\kappa$																			
$1^{++}$	$A_1$	D	?	$Q^A$																			
$1^{+-}$	B	$h^\omega$	$h^\phi$	$Q^B$																			
$2^{++}$	$A_2$	f	$f'$	$K^{*1}$																			

$L=2$	{	<table style="border-collapse: collapse; width: 100%; text-align: center;"> <tr> <td style="padding: 2px 10px;"><math>1^{--}</math></td> <td style="padding: 2px 10px;"><math>\rho'</math></td> <td style="padding: 2px 10px;">?</td> <td style="padding: 2px 10px;">?</td> <td style="padding: 2px 10px;">?</td> </tr> <tr> <td style="padding: 2px 10px;"><math>2^{--}</math></td> <td style="padding: 2px 10px;"><math>F_1</math></td> <td style="padding: 2px 10px;">?</td> <td style="padding: 2px 10px;">?</td> <td style="padding: 2px 10px;">?</td> </tr> <tr> <td style="padding: 2px 10px;"><math>2^{-+}</math></td> <td style="padding: 2px 10px;"><math>A_3</math></td> <td style="padding: 2px 10px;">?</td> <td style="padding: 2px 10px;">?</td> <td style="padding: 2px 10px;">L</td> </tr> <tr> <td style="padding: 2px 10px;"><math>3^{--}</math></td> <td style="padding: 2px 10px;">g</td> <td style="padding: 2px 10px;"><math>\omega'</math></td> <td style="padding: 2px 10px;"><math>\phi'</math></td> <td style="padding: 2px 10px;"><math>K^{*11}</math></td> </tr> </table>	$1^{--}$	$\rho'$	?	?	?	$2^{--}$	$F_1$	?	?	?	$2^{-+}$	$A_3$	?	?	L	$3^{--}$	g	$\omega'$	$\phi'$	$K^{*11}$	(●)
$1^{--}$	$\rho'$	?	?	?																			
$2^{--}$	$F_1$	?	?	?																			
$2^{-+}$	$A_3$	?	?	L																			
$3^{--}$	g	$\omega'$	$\phi'$	$K^{*11}$																			

A few comments are in order:

- there are candidates for each of the  $J^{PC}$  multiplets, for each of the quark model supermultiplets; the  $L = 0$  supermultiplet is complete, the  $L = 1$  is almost complete (although there are some reservations about the diffractively produced states in the  $1^{++}$  and  $1^{+-}$  nonets), while the  $L = 2$  system has only the bare bones showing at present.
- the  $I = 0$  states are a real "disaster area", and need a lot of work. For the magically mixed states (see Fig. 9:  $1^{--}$ ,  $1^{+-}$ ,  $2^{++}$ ,  $2^{--}$ ,  $3^{--}$ ), the " $\phi$ " meson may be expected to couple more strongly to  $K^-$ -induced reactions than to  $\pi$ -induced reactions, in analogy to the observed  $\phi$  production.<sup>24</sup> (See Fig. 10.) In this case the  $K^-$  cross section is  $\sim 50$  times greater than the  $\pi$  cross section. These " $\phi$ -like" states will decay to  $K\bar{K}$  (except for  $1^{++}$ ,  $1^{+-}$ ,  $2^{--}$ ,  $2^{-+}$  which are forbidden),  $\bar{K}K^*$  and  $K^*K^*$ . The non-strange quark,  $I = 0$  states should couple to channels like  $\pi^0\rho^0$ ,  $\pi\delta$ ,  $\pi\omega$ ,  $\pi A_2$ .
- the  $A_1$  and  $Q$  states are another problem area, as we heard in the talks by Ascoli,<sup>19</sup> Lasinski<sup>20</sup> and Jones.<sup>25</sup> We expect mesons with the quantum numbers and the masses of these diffraction produced enhancements to complete the quark model classification scheme discussed above. However, no resonant-like behavior of the  $1^+$  phase is observed for either the  $(3\pi)^{19}$  or  $(K\pi\pi)^{26}$  systems in the various amplitude studies which have been reported. The usual plea is to study these states in non-diffractive processes;

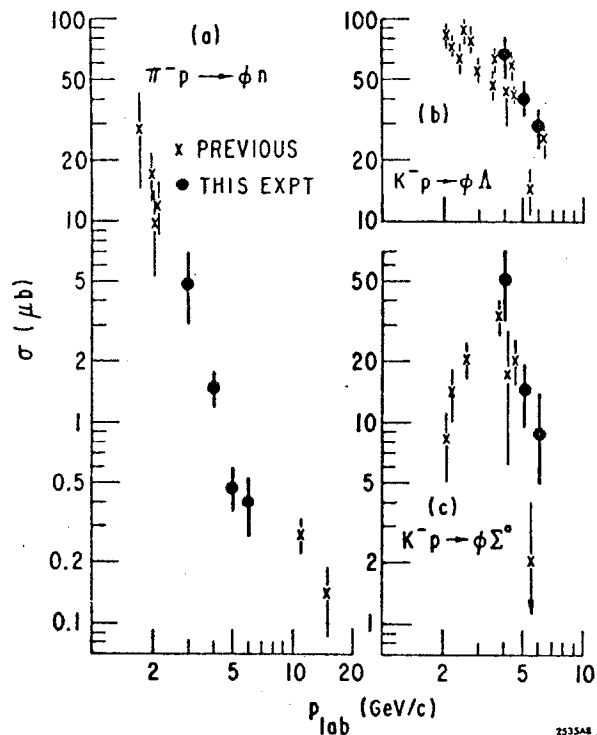
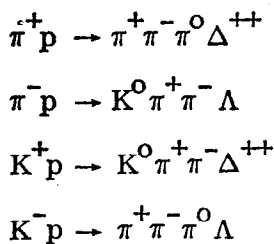
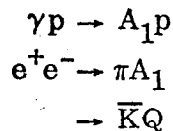


FIG. 10--The cross sections for  $\phi$ -meson production by  $\pi^- p$  and  $K^- p$  collisions.

However, the high multiplicity of these final states and the small cross sections make them non-trivial experiments. I will comment below on two other reactions which may be favorable for the study of  $A$  or  $Q$  production,



All of these experiments become more accessible with the new tools we will discuss below.

The typical reactions to be studied in searching for the missing states of in Fig. 9 are listed in Table III. Many of the reactions involve 4, 5, or 6 charged particles which would be an impossible situation for the present generation of forward magnet spectrometers,<sup>27</sup> which have been so successful for the two and three body final state analysis. The new multiparticle spectrometers to be discussed below should be capable of handling these inelastic reactions. There is a whole body of other reactions involving two or more neutrals (e.g.  $\pi^0 n$ ,  $\omega \eta$  etc.) which will require additional photon and neutron detectors — but the present instrumentation for the new spectrometers is sufficient to open up a wide vista of important and interesting new channels for PWA.

Table III Typical inelastic hadron reactions to be studied with new multiparticle spectrometers.

Decay Mode	Reaction	
$\pi\pi$	$\pi^- p \rightarrow \pi^+ \pi^- n$	S I M I L A R
$K\bar{K}$	$\rightarrow K^+ K^- n$	
$\pi^0 \rho^0$	$\pi^- p \rightarrow \pi^+ \pi^- \pi^0 n$	
	$\pi^+ p \rightarrow \pi^+ \pi^- \pi^0 \Delta^{++}$	M O D E S
$\pi\omega$	$\pi^- p \rightarrow \pi^- \pi^+ \pi^- \pi^0 p$	
$\pi\phi$	$\pi^- p \rightarrow \pi^- K^+ K^- p$	F O R
$\rho\rho$	$\pi^- p \rightarrow \pi^+ \pi^- \pi^+ \pi^- n$	
	$\pi^+ p \rightarrow \pi^+ \pi^- \pi^+ \pi^- \Delta^{++}$	K*
$\pi\pi_N$ } $\pi B$ }	$\pi^+ p \rightarrow \pi^+ \pi^- \pi^+ \pi^- \pi^0 \Delta^{++}$	K $\pi$
		K $\phi$
$\pi A_2$	$\left\{ \begin{array}{l} \pi^+ p \rightarrow \pi^+ \pi^- \pi^+ \pi^- \Delta^{++} \\ \pi^- p \rightarrow \pi^+ \pi^- \pi^+ \pi^- n \end{array} \right.$	K $\rho$
		K $\omega$
		K $\pi_N$
$K\bar{K}^*$	$\pi^+ p \rightarrow K^+ \bar{K}^0 \pi^- \Delta^{++}$	KA <sub>2</sub>
	$\rightarrow K^0 K^- \pi^+ \Delta^{++}$	K* $\pi$
$K^* \bar{K}^*$	$\pi^- p \rightarrow K^+ \pi^- K^- \pi^+ n$	K* $\omega$
	$\rightarrow K^0 \pi^+ \bar{K}^0 \pi^- n$	$\bar{\Delta} p$

generation of forward magnet spectrometers,<sup>27</sup> which have been so successful for the two and three body final state analysis. The new multiparticle spectrometers to be discussed below should be capable of handling these inelastic reactions. There is a whole body of other reactions involving two or more neutrals (e.g.  $\pi^0 n$ ,  $\omega \eta$  etc.) which will require additional photon and neutron detectors — but the present instrumentation for the new spectrometers is sufficient to open up a wide vista of important and interesting new channels for PWA.

As the study of meson states progresses to higher masses, several difficulties befall the conventional experimental tools:

- the cross section for production of the states becomes smaller and smaller;
- the total width becomes larger, and the elastic width becomes smaller; (this makes it more essential to use partial wave analysis techniques to search out the resonant structure, and eventually forces the study of inelastic channels to obtain information on these high mass states — see Fig. 11;
- the spin of the leading particle states becomes higher, resulting in more and more

of the production cross section peaking in the very forward (backward) direction — just the region in which the acceptance of the conventional forward spectrometers is poorest;<sup>28</sup>

- the multiplicity of the decay becomes larger, causing problems for the efficient detection of all the final state particles, and also for the design of a good, selective trigger.

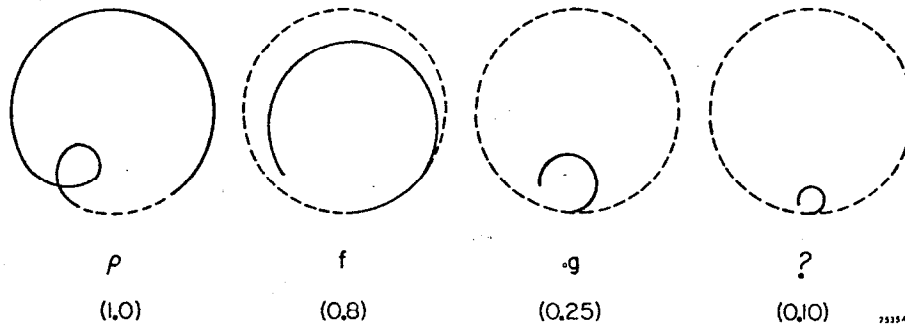


FIG. 11--Argand plots for the elastic scattering amplitude for four resonances with  $x_{e1} = 1.0, 0.8, 0.25$  and  $0.10$ .

Finally, a comment on the statistics required for experiments attempting an amplitude (or partial wave) analysis of inelastic reactions. From the LBL-SLAC  $s$ -channel<sup>6</sup>  $N^*$  studies we know that  $\sim 10,000$  events per mass bin are required to find a unique solution for a problem with 60 partial waves. As the statistics are reduced ambiguous solutions appear and typically for an experiment with  $\sim 2000$  events per bin, two or three different solutions were found. We use this lower estimate of the number of events required to set a scale for the new experiments, and hope that continuity constraints will allow selection of the unique fit from the several ambiguous alternatives.

Suppose now we want to study the process  $\pi \rightarrow 3\pi$  over a 2000 MeV region of  $(3\pi)$  mass, in 20 MeV bins and with 2-3 bins in momentum transfer (to see the production mechanism); this study will require an experiment of  $\sim 1000$  events/ $\mu\text{b}$  for a diffractive process, or  $\sim 7-10,000$  events/ $\mu\text{b}$  for a non-diffractive reaction. A similar experiment is shown in Fig. 12, where the

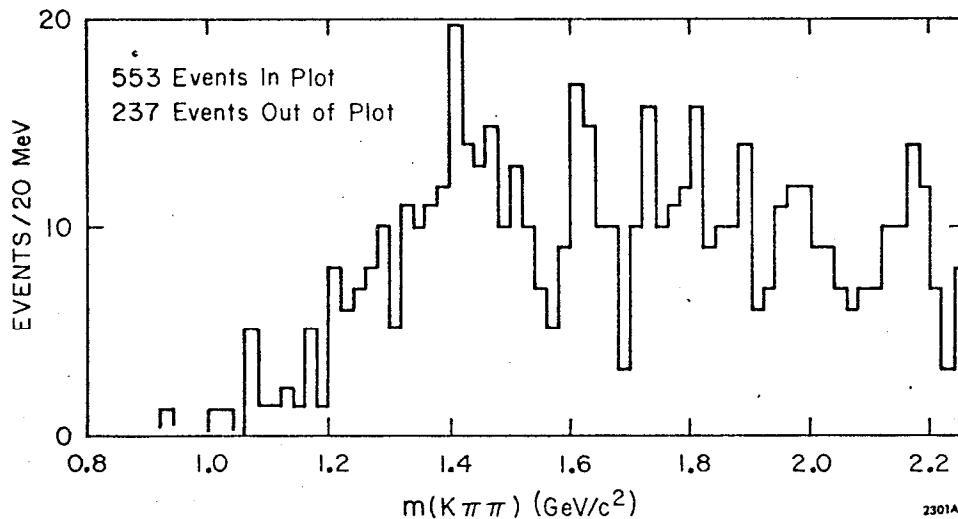


FIG. 12--The effective mass spectrum of  $(K\pi\pi)$  from the reaction  $K^+p \rightarrow (K\pi\pi)\Delta^{++}$  at  $10 \text{ GeV}/c$ .

mass spectrum for charge exchange  $K \rightarrow K\pi\pi$  is shown from a 10 GeV/c  $K^+p$  HBC experiment.<sup>29</sup> This experiment has a sensitivity of  $\sim 20$  events/ $\mu\text{b}$ ; so to obtain our 2000 events/20 MeV mass bin and with 2-3 t bins, we require a  $K^+p$  experiment of  $\sim 10,000$  events/ $\mu\text{b}$  sensitivity to successfully perform an amplitude study of the non-diffractive ( $K \rightarrow K\pi\pi$ ) scattering.

To summarize, new progress in understanding meson spectroscopy requires:

- systematic, high statistics experiments;
- partial wave analysis in 2-body and multi-body scattering to identify the full resonance structure and determine the properties (e.g. mass, width, spin, parity, isospin, coupling signs and branching ratios);
- typical decay modes to be studied -  $\pi\delta$ ,  $\pi\rho$ ,  $\pi\omega$ ,  $\pi A_2$ ,  $\bar{K}K^*$ , (i.e. multiparticle final states);
- sensitivity required - 1000 events/ $\mu\text{b}$  for diffractive processes  
10,000 events/ $\mu\text{b}$  for non-diffractive processes;
- need detectors with good geometrical acceptance, capable of handling high multiplicity final states and with high data rate capacity to accomplish  $10^4$  events/ $\mu\text{b}$  experiments in a reasonable amount of calendar and accelerator time.

### C. The New Tools.

In this section I want to briefly describe several new areas of opportunity in experimental meson spectroscopy and the physics they should impact - (a) new detectors, (b) photon beams, (c)  $e^+e^-$  storage rings.

(a) New detectors. There is a new generation of multiparticle spectrometers becoming available - the MPS system at BNL, OMEGA at CERN and LASS at SLAC. The MPS and OMEGA set-ups have been described in detail before,<sup>30</sup> so I will only briefly remind you of them. The general layout of these spectrometers is shown in Fig. 13. Both are large aperture magnets with  $\sim 1.5$  meters gap and large field volume for the detection and measurement of the secondary tracks. In both cases, the sides of the magnet (the iron flux return path) may be moved and restacked in a flexible geometry to allow specific particle orbits to exit the system, or to insert special purpose instrumentation. The liquid hydrogen target in both systems is positioned within the field volume and is surrounded by spark chambers. The BNL spark chamber system is completely digitized, while the Omega has T.V. camera readout of optical spark chambers. Both are high data rate devices, capable of logging (30-50) events/sec. and of being triggered on highly selective event samples. The types of triggers available at present are slow proton and neutron recoils, fast forward p,  $\bar{p}$  or  $K^\pm$  and forward produced  $V^0$ . Multiwire proportional chambers are being built to provide even more flexible triggers. Particle identification is provided by large Cerenkov counters positioned downstream. Both spectrometers are capable of doing  $10^3$ - $10^4$  event/ $\mu\text{b}$  experiment in a typical 10-day accelerator period.

A new multiparticle spectrometer is currently being assembled at SLAC - LASS - it is shown schematically in Fig. 14. Since it is new and the basic philosophy is somewhat different from the above spectrometers, I will describe it more fully. It is a two magnet system with a conventional forward magnet spectrometer and a target vertex detector. The forward system is the classic field-free "spark chamber - large aperture magnet - spark chamber" geometry, which has proved so powerful (in terms of data rate and resolution) and so economical (in terms of computer time) in the  $\pi\pi \rightarrow \pi\pi$  and  $K\pi \rightarrow K\pi$  experiments at CERN, ANL and SLAC. The magnet has a 2 meter  $\times$  1 meter gap

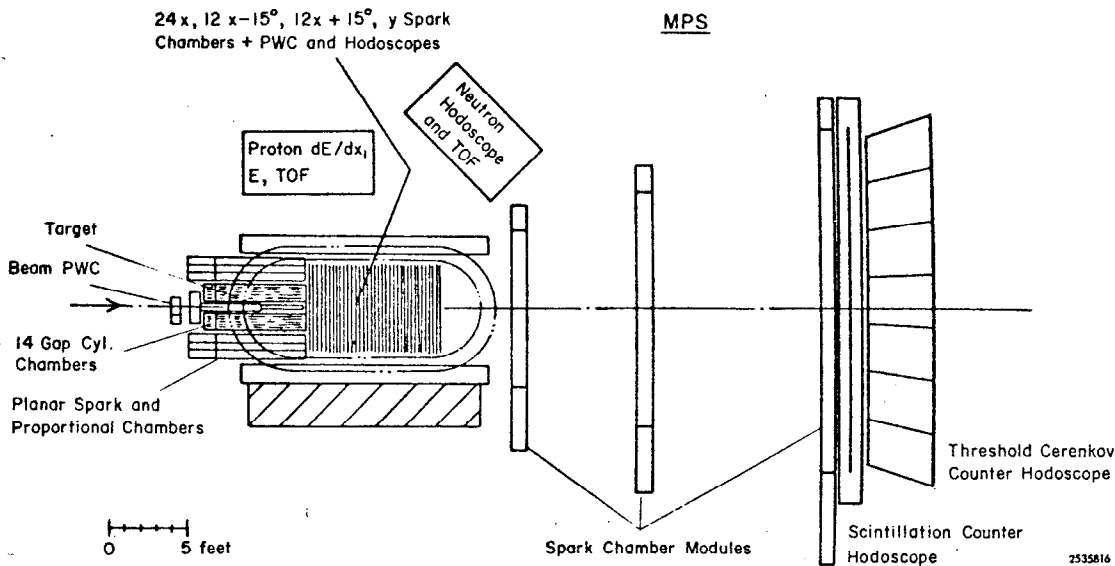
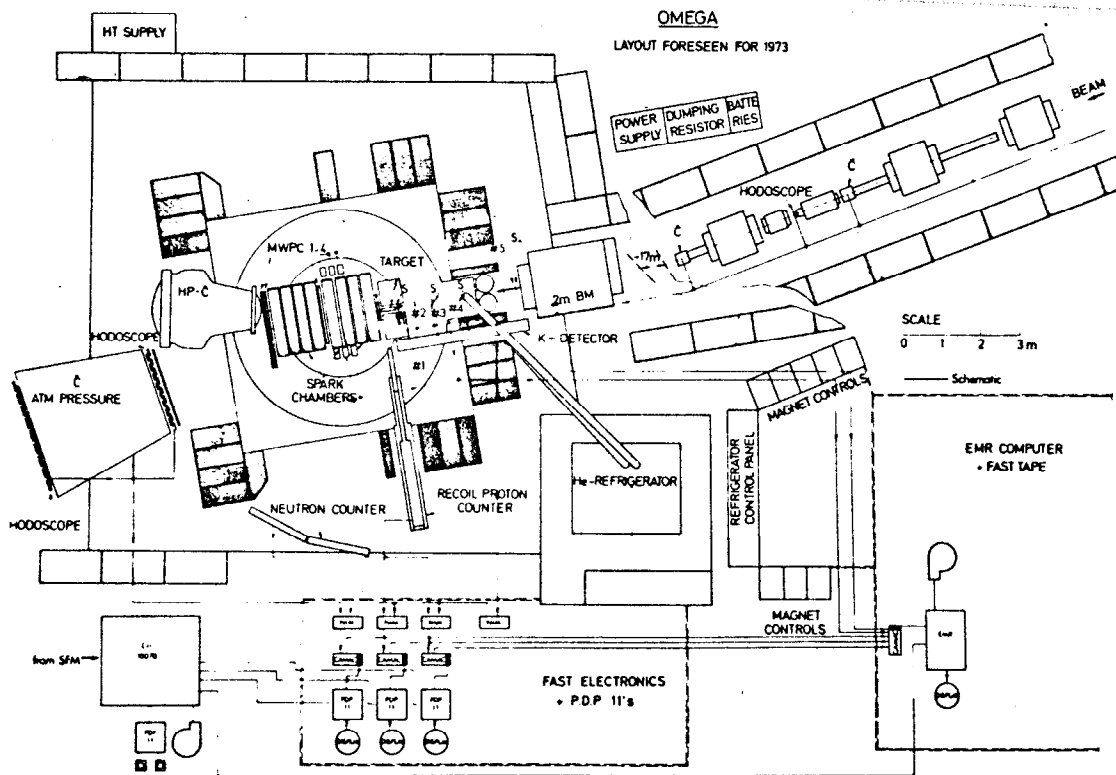


FIG. 13--The layout of the (a) OMEGA, (b) MPS spectrometer facilities.

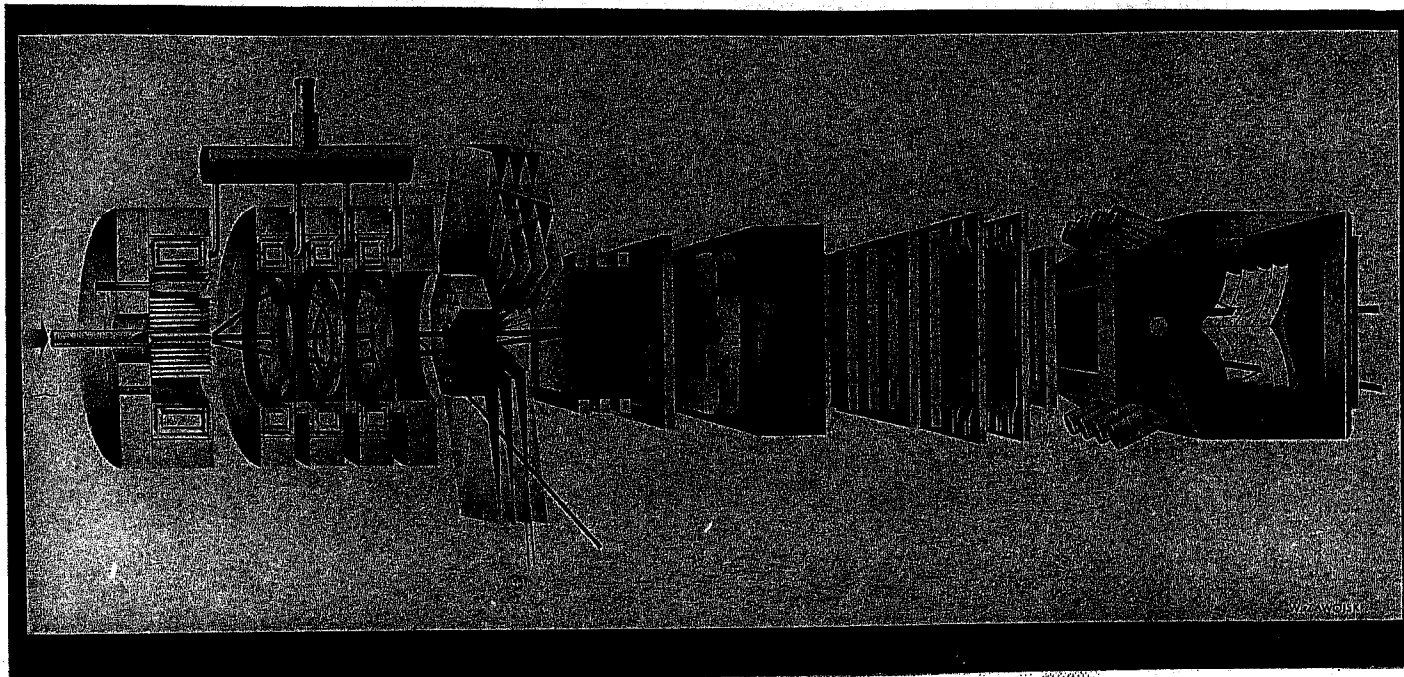


FIG. 14--A schematic of the SLAC LASS system.

with 30 kG m analyzing field integral. The design of the vertex detector was chosen to be as non-interfering with the forward system, (i.e. as orthogonal in measurement space), as possible. The magnet is a superconducting solenoid, 2 meters in diameter and 3-1/2 meters long with the 25 kG magnetic field parallel to the beam. This configuration does not interfere with the small angle fast tracks, (the peripheral particles), which are measured downstream (since the momentum vector is essentially parallel to the magnetic field) but measures well the large angle tracks and the slow tracks missed by the forward system.

The particle identification is provided by two threshold Cerenkov counters — an atmospheric pressure counter, with 37 separate cells, mounted at the end of the solenoid, and a 3 atmosphere pressure counter with 8 cells positioned at the end of the downstream system. The detectors are a varied mixture of techniques — downstream they are magneto-strictive spark chambers, while in the solenoid and between the two magnets, they are capacitive read-out spark chambers and proportional wire chambers. This system, which is directly on-line to an IBM 370/168 computer, is designed for high data rates, and is able to handle up to 100 events/sec.

The LASS system may be triggered on the forward multiplicity, recoil proton or forward produced  $V^0$ . In addition, two novel triggers are being prepared which deserve further description: (1) the solenoid-axial field causes the secondary particles to sweep out a helical trajectory, whose diameter is related to  $P_T$  and whose pitch is related to  $P_L$ .  $P_T$  and  $P_L$  are directly measured using the induced signal from three proportional wire chamber wheels, where the high voltage planes have been etched to give polar coordinate,  $(R, \theta)$ ,

information (i. e. the pitch and radius of the trajectory is available digitally). Thus, trigger arrangements may be devised to select specific regions of  $P_T$  or  $P_L$  or both; (2) the data acquisition system has an inbuilt pause of (3-10) msec. before committing an event to tape, during which time the full arithmetic power of the IBM 370/168 may be brought to bear on making decisions to accept or reject the event, or to set a flag for the control of subsequent analysis. One feature of this setup which should provide a powerful trigger is that effective masses of recoil particles may be calculated in real time, using the digital information from the proportional chambers surrounding the target and immediately downstream. For example, the effective mass of a recoil  $\Lambda(\rightarrow p\pi^-)$  or  $\Delta^{++}(\rightarrow p\pi^+)$  can be calculated within the 10 msec pause, with an accuracy of  $\sim 100$  MeV.

The performance and general characteristics of these new devices is summarised in Table IV.

Table IV Summary of MPS, OMEGA and LASS characteristics

MPS (operate in summer 1974)	OMEGA (currently operating)	LASS (operate in fall 1974)
Target in Field Volume and Surrounded by Spark Chambers		
45 kG meters of analysis	54 kG meters of analysis	30 kG meters + 87 kG meters of longitudinal field
35 events/sec	50 events/sec	(40 - 100) events/sec
$\leq 9$ GeV/c separated	$\leq 15$ GeV/c unseparated	$\leq 16$ GeV/c separated
Forward Particle Identification by Downstream Cerenkov Counters		
Triggers: <ul style="list-style-type: none"> <li>● Recoil Proton</li> <li>● Forward <math>V^0</math></li> <li>● Forward Multiplicity</li> <li>● <math>2V^0</math></li> <li>● Recoil Neutron</li> </ul>	<ul style="list-style-type: none"> <li>● Recoil Proton</li> <li>● Recoil Neutron</li> <li>● Fast <math>V^0</math></li> <li>● Forward K, p</li> </ul>	<ul style="list-style-type: none"> <li>● Recoil Proton</li> <li>● Recoil <math>\Delta^{++}</math></li> <li>● Forward Multiplicity</li> <li>● Forward <math>V^0</math></li> <li>● <math>P_T, P_L</math></li> </ul>

These new devices represent new opportunities for meson spectroscopy with

- almost  $4\pi$  acceptance spectrometers,
- good multiparticle detection efficiency,
- high data rate capability (making  $10^3$ - $10^4$  event/ $\mu$ b experiments possible),
- good measurement resolution,
- particle identification,
- a variety of trigger options
  - recoil p, n,  $\Lambda$ ,  $\Delta^{++}$
  - forward  $K^\pm, p^\pm$
  - forward multiplicity
  - $P_T, P_L$

(b) Photon Interactions Photon beams should be an important tool in meson spectroscopy, since the photon is the only stable meson with spin 1. The techniques for making polarized, and even monochromatic photon beams are now well established.<sup>31</sup> One may even study photoproduction with longitudinally polarized photons, using the virtual exchange in inelastic lepton scattering. We may also probe subnuclear structure using the Primakoff effect, which should be a very characteristic signal and quite accessible at high energies; these possibilities were reviewed by Rosen<sup>32</sup> at this meeting. The photon couplings can also be investigated in the study of  $e^+e^-$  collisions, which are dominated by the one photon exchange intermediate state; I will talk more of this in a moment.

Historically, the photoproduction experiments<sup>33</sup> have taught us a great deal of reaction dynamics, from the beautiful studies of  $\rho$ ,  $\omega$ ,  $\phi$  production. However, these experiments, large as they were, have not been sensitive enough to probe new meson structure; typical sensitivity has been  $\sim 500$  events/ $\mu\text{b}$  while non-diffractive meson production is expected to have a cross section  $\sim 0.1 \mu\text{b}$  at energies  $\sim 10$  GeV. Typical reactions to be studied are listed in Table V; from the quark model calculations of Gilman and Karliner,<sup>34</sup> the cross sections for all these processes are predicted to be approximately equal.

Table V Some interesting photoproduction reactions

$\gamma p \rightarrow A_2^+ \Delta^0$	$\rightarrow \pi^+ \pi^+ \pi^- p \pi^-$
$(\gamma n \rightarrow A_2^- p)$	$\rightarrow \pi^- \pi^+ \pi^- p$
$\gamma p \rightarrow A_1^+ \Delta^0$	$\rightarrow \pi^+ \pi^+ \pi^- p \pi^-$
$\gamma p \rightarrow B^+ \Delta^0$	$\rightarrow \pi^+ \pi^+ \pi^- \pi^0 p \pi^-$
$\gamma p \rightarrow h^0 p$	$\rightarrow \pi^+ \pi^- \pi^0 p$
$\gamma p \rightarrow \delta^+ \Delta^0$	$\rightarrow \pi^+ \pi^+ \pi^- \pi^0 p \pi^-$
$\gamma p \rightarrow f p$	$\rightarrow \left( \begin{array}{c} \pi^+ \pi^- \\ \pi^+ \pi^- \pi^+ \pi^- \\ K^+ K^- \end{array} \right) p$
$\gamma p \rightarrow f' p$	$\rightarrow K^+ K^- p$
$\gamma p \rightarrow D^0 p$	$\rightarrow \pi^+ \pi^- \pi^+ \pi^- \pi^0 p$

Typical Cross Section at  $10^4 \text{ GeV}/c \sim 0.1 \mu\text{b}$

The OMEGA and LASS spectrometers will both embark on experimental programs in photon beams during the next few years. At CERN, the OMEGA facility will use a tagged, polarized photon beam from the SPS.<sup>35</sup> The beam will allow study of photoproduction reactions in the range (10-60) GeV, with useful polarization information in the (30-50) GeV range, and with sensitivities of a few  $10^4$  events/ $\mu\text{b}$ . The beam parameters are summarized in Fig. 15.

LASS has a unique property for photon and electron beam experiments. In the past the main problem for these experiments has been that the electromagnetic background is many orders of magnitude larger than the hadronic cross sections. This background is characterized by having  $q^2=0$ , which means in the solenoid there is no net bending, and therefore, all the background is maintained in a tight bundle on the beam axis. As this background emerges from the solenoid we will perhaps have to "drain" the downstream system using a superconducting tube to exclude the magnetic field

from the beam region similar to the one described at the last meson conference by Martin.<sup>36</sup> In these conditions we expect to be able to study

photoproduction processes in the (5-20) GeV range, with useful polarization around 15 GeV, with a sensitivity of  $\sim 10^4$  events/ $\mu$ b/day.

Another interesting study of meson production with photons concerns the helicity structure in the  $\rho\pi$ ,  $\omega\pi$  decays. For example, we know the decay

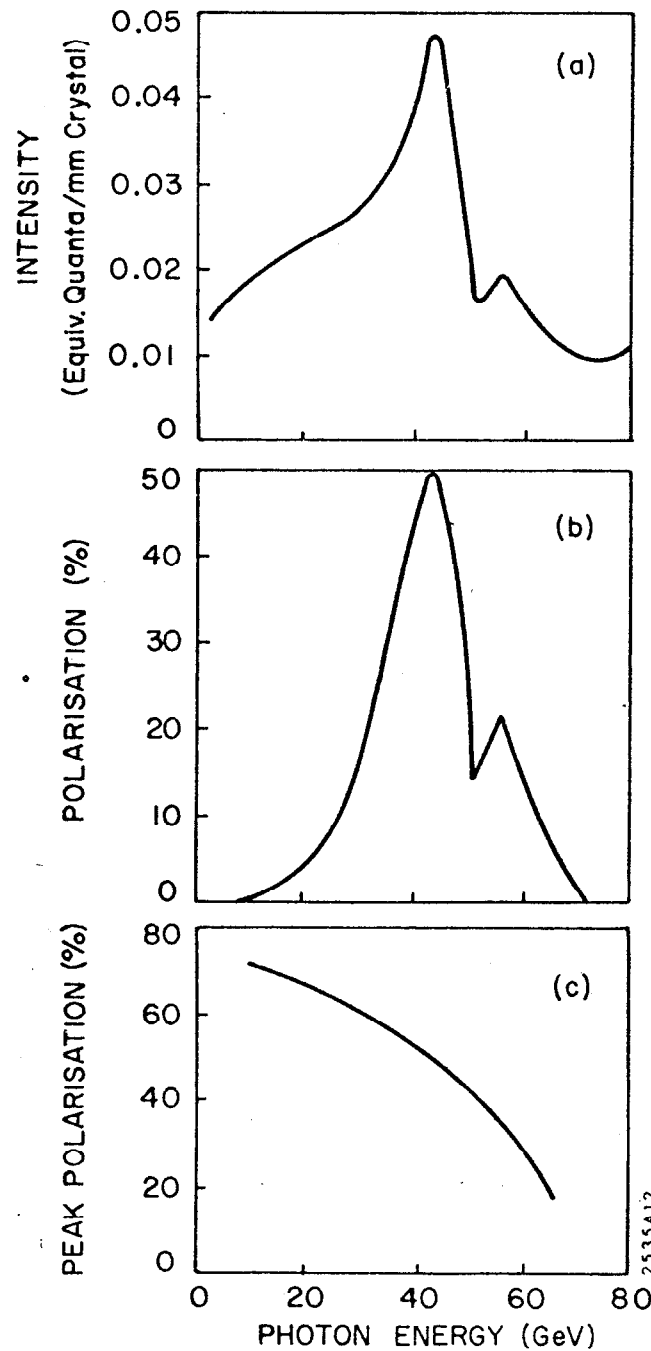


FIG. 15--The intensity and polarization parameters from the profused photon beam for the OMEGA experiments at the CERN SPS.

$A_1 \rightarrow \rho\pi$  has dominantly longitudinal  $\rho$ 's, and  $B \rightarrow \omega\pi$  produces dominantly transverse  $\omega$ 's. Thus, B mesons should be strongly observed with real photons while  $A_1$  production should be enhanced using longitudinal photons from inelastic electron scattering. (See Fig. 16.)

We expect many higher mass mesons to couple to the vector mesons, and this trick of using real or virtual photons may be important in their production and will certainly be interesting for studying the helicity structure of their decays.

(c) Electron-Positron Storage Rings

In the last few years we have seen a new area of physics opened up with the effective operation of electron-positron colliding beam facilities. These new tools allow the study of meson spectroscopy through three different processes — (i) the s-channel formation of meson states in  $e^+e^-$  collisions, (ii) the production of meson states in  $e^+e^-$  multiparticle collisions, and (iii) the utilization of the two photon process to form mesonic states in s-channel  $\gamma\text{-}\gamma$  collisions. The characteristics of operating (and proposed) storage ring machines are shown in Fig. 17, where the total energy in the center of mass of the  $e^+e^-$  collision is plotted against the luminosity of the accelerator.

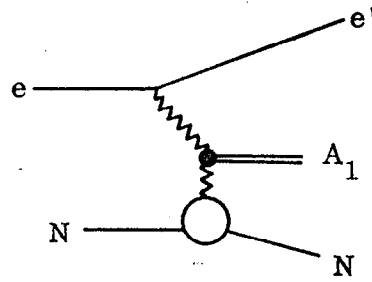


FIG. 16--Diagram for inelastic electroproduction of  $A_1$  meson.

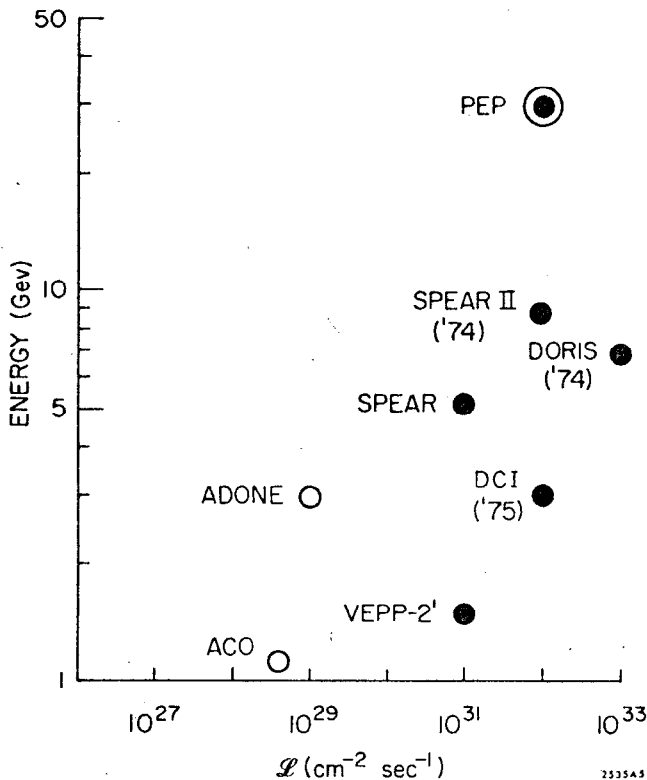


FIG. 17--The present and proposed  $e^+e^-$  colliding beam facilities.

Let us consider each of the three  $e^+e^-$  processes in turn.

(i) The old generation of storage ring machines (viz. ACO, ADONE, and VEPP) have performed extremely elegant experiments on the study of s-channel formation of the leading vector mesons —  $\rho$ ,  $\omega$ , and  $\phi$  — through the one photon annihilation process —

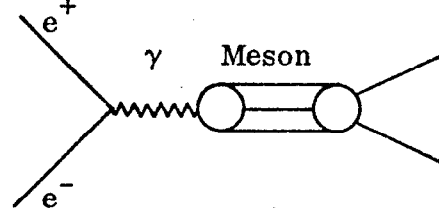


FIG. 18--Formation of meson resonance in  $e^+e^-$  s-channel process.

As the total center of mass energy is varied by changing the energy of the stored  $e^+e^-$  beams, the experiments scan a range of meson mass and look for an

enhancement in the cross section of a given final state. Such an enhancement is interpreted as evidence for the formation of a resonant state, with the same quantum numbers as the photon, (viz.  $J^{PC} = 1^{--}$ ). Evidence of other vector mesons, one at 1600 MeV (the  $\rho'$  (1600)), and possible signs of another structure at 1250 MeV, have been reported by groups at ADONE,<sup>37</sup> but all three of these older machines are very limited by their luminosities (i.e. the flux of colliding electrons). The new generation of accelerators — VEPP 2', and DCI facility in Paris — should allow for a detailed scan for new  $1^-$  states up to masses of 3000 MeV, with  $10^2$ - $10^3$  times the sensitivity. In addition to studying  $\pi\pi$  and  $K\bar{K}$  channels it should be interesting to look for new vector mesons coupling to inelastic channels like  $\pi\rho$ ,  $\pi\omega$ ,  $\pi A_2$ ,  $\bar{K}K^*$ ,  $\pi B$ , etc.

(ii) The production of meson resonances ought to be a very profitable hunting ground for the new  $e^+e^-$  facilities — SPEAR I, II and DORIS. (See Fig. 17). We know many states which couple strongly to vector mesons, (see Table VI), and would expect to see such states produced in  $e^+e^-$  collisions through the following diagram:

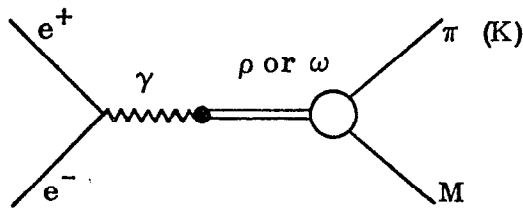


FIG. 19--Production of a meson resonance in  $e^+e^-$  multiparticle process.

Such a reaction would be an interesting place to study the  $A_1$ ,  $Q$  question, as they should be seen in

$$e^+e^- \rightarrow \text{"}\rho\text{"} \rightarrow \pi A_1 \\ \rightarrow \bar{K}Q .$$

Table VI Examples of Mesons decaying to Vector Meson

$\omega \rightarrow \rho\pi$
$\pi_N \rightarrow \rho\pi$
$\phi \rightarrow \rho\pi$
$A_1 \rightarrow \rho\pi$
$B \rightarrow \omega\pi$
$A_2 \rightarrow \rho\pi$
$g \rightarrow \omega\pi$
Also $Q \rightarrow K\rho$
$K_{1420} \rightarrow K\rho$

and the supposed  $J=3,4 K^*$  also couple to  $K\rho$ .

Since we know that the decay chain  $\omega \rightarrow \rho\pi$  provides a good description of  $\omega \rightarrow 3\pi$  decay characteristics, we may take the  $e^+e^- \rightarrow \text{"}\rho\text{"} \rightarrow \omega\pi$  cross section as setting a scale for the other processes listed in Table VI. Taking this cross section ( $\sigma(\omega\pi) \sim 2 \cdot 10^{-32} \text{ cm}^2$  at threshold), and going (500-1000) MeV above threshold to kinematically separate the recoiling particles and assuming an  $E^{-6}$  fall-off of the exclusive cross section still leaves a yield of many thousands of events per day at DORIS. Both DORIS and SPEAR have large, nearly- $4\pi$  magnetic detectors which should be ideal for these studies.

(iii) Although the single photon intermediate state dominates  $e^+e^-$  processes, there is considerable interest in studying the two photon exchange process.

The amplitude for this process is down by  $\alpha^2$  compared to the single photon channel, but at high energies it

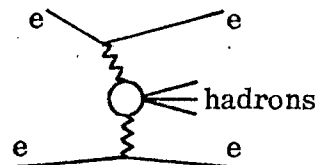


FIG. 20--Formation of a meson state in s-channel  $\gamma\text{-}\gamma$  collision.

begins to compete and becomes an attractive tool in its own right, since the cross section is enhanced by factors of  $\ln^2(E/m_e)$ . The cross section for the process shown in Fig. 20 has been calculated,<sup>38</sup> and predicts reasonable event rates for SPEAR II, and especially PEP energies (see Fig. 17). The cross sections are shown for three meson mass regions in Table VII.

Table VII Two-Photon Cross Sections

Mass	Cross Section ( $10^{-33} \text{ cm}^2$ )	
	( $2 \times 3 \text{ GeV}$ )	( $2 \times 15 \text{ GeV}$ )
(300-1000)	11	30
(1000-2000)	1.7	6.9
(2000-6000)	0.6	5.1

For  $\mathcal{L} \sim 10^{32}$ , expect yield of  
 1000 < M < 2000 hadrons, to be  
 ~6,000/day at SPEAR II  
 and ~25,000/day at PEP energies.

These are basically experiments on  $\gamma\text{-}\gamma$  scattering and therefore allow study of mesons with  $C = +1$ . The two photon initial state couples to spin-parity multiplets  $0^{++}, 2^{++}, 2^{-+}$ . (Since the two photons are almost real, they cannot couple to  $J = 1$  systems.) Such experiments would allow further study of the confusing  $\delta, \epsilon, S^*$  states in the  $L = 1, 0^{++}$  multiplet, and clarify their relationship to the  $\epsilon'$ , the other s-wave  $\pi\text{-}\pi$  state under the f-meson. In addition, these experiments should allow investigation of the diffractive enhancement called the  $A_3$  (— the Regge recurrence of the pion), in a non-diffractive reaction.

These experiments are very difficult in that the recoil electrons must be detected in addition to the final hadronic products. As so often is the case in storage ring experiments, this requires a close coupling between the design and operation of the storage ring and the experiment itself. Both DORIS and PEP have been designed with such experimental programs in mind. It should be an interesting and profitable area of experimental meson spectroscopy.

Experience from SPEAR is not too encouraging, as far as meson spectroscopy is concerned, as we heard from Chinowsky<sup>39</sup> — the exclusive cross sections fall very fast and there is little resonance structure seen. However, at present the mass resolution is not very good ( $\sim 40 \text{ MeV}$ ), and the statistics are very poor. Many of you may remember the first results of high energy  $pp \rightarrow$  many  $\pi$ 's were thought to be completely phase-space-like. Only when much work had been done on these channels and very high statistics were finally achieved did it become clear that the final states were resonance dominated. The resonant signal had been swamped by the diluting effect of the large number of combinations per event in the mass plots. I think for the moment the data is too sparse and the promise too great not to continue to look in  $e^+e^-$  annihilation for more information on meson resonances.

## TOWERS OF MESONS

In this section I would like to point out that the empirical evidence for the existence of towers of meson states is strengthening. In Fig. 21, the Chew-Frautschi plot for the natural parity mesons is displayed, showing the  $\rho, f, g$ -meson leading trajectory, and below it I have circled several fairly established states —  $\epsilon, \delta, \rho'$ , and others somewhat more speculative —  $\epsilon'$ , the s-wave  $\pi\text{-}\pi$  effect under the f-meson;<sup>40</sup> an  $f\pi$  effect around a mass of 1750 MeV seen in the  $2^+$  wave in the Ascoli analysis of  $(\pi \rightarrow 3\pi)$  scattering;<sup>19</sup> a  $1^-$  effect

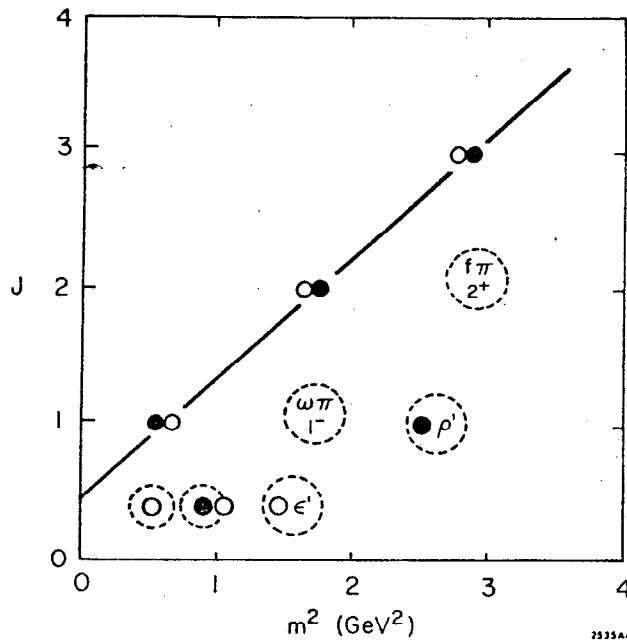


FIG. 21--Chew-Frautschi plot for the natural parity mesons.

f-mesons. Table VIII shows the kind of structure which would be expected in this model, and marked as circles are the possible daughter candidates. An alternative view is offered in the quark model, where in addition to the  $L=0, 1, 2$  --, supermultiplets discussed in Section III above, one expects radial excitations to appear. Evidence for radial excitations in the baryon system is growing with the reporting of the observation of the first and second radial excitations of the proton.<sup>7</sup> Such a possibility for the mesons is outlined in Fig. 23. It is not our purpose to decide which picture is correct, but to point out that an interesting structure of lower lying states is emerging from our meson studies.

Further support for these suggestions comes from studies of  $\pi\pi \rightarrow \bar{N}N$  and  $\bar{N}\bar{N} \rightarrow \pi\pi$ . In Fig. 24, the results of an analysis by Hyams et al.<sup>42</sup> on  $\pi^-p \rightarrow \bar{p}p\pi$  are presented. They tried to fit the complicated structure in the  $\bar{p}p$  angular distributions by allowing a resonance plus background in each partial wave up to  $\ell = 6$ . The "resonances" resulting from this fit are shown on the Chew-Frautschi plot together with results from analysis of  $\bar{N}N \rightarrow \pi\pi$ . The purpose is not to claim any specific spectroscopic states from these analyses, but to draw attention to the possible existence of structure below the leading trajectory and the formation of towers of states.

One final comment on the influence of the angular momentum barrier on studies of low lying states such as those discussed above. Figure 25 shows a Chew-Frautschi plot with the leading trajectory, and the curve  $J \propto k \cdot R$ . Here  $J$  is the total angular momentum of the  $\pi-\pi$  state and is taken as being proportional to the product of the center of mass momentum of the pion times their spatial separation,  $R$ , which is known to be  $\sim 1$  fermi for non-diffractive hadronic amplitudes. We are all familiar with the inhibition of high mass leading particles coupling to the elastic channel due to the angular momentum

near the f-meson coupling to  $\omega\pi$ , which has been suggested in an ADONE experiment reported at this meeting,<sup>37</sup> and the SLAC-LBL back-scattered laser beam experiment.<sup>41</sup>

Such a tower structure receives tentative support from recent results on high mass  $\pi-\pi$  phase shifts from the CERN-MUNICH group, discussed by Manner.<sup>15</sup> One of their four possible solutions shows structure in the s-, and p-waves below the f-meson and in the s-, p- and d-waves below the g-meson (see Fig. 22).

Similar regularities have been expected in various theories. The Veneziano model predicts many daughters of alternating I-spin and parity, which were originally introduced to kill the non-observed backward peak in  $\pi-\pi$  scattering in the region of the  $\rho$ - and

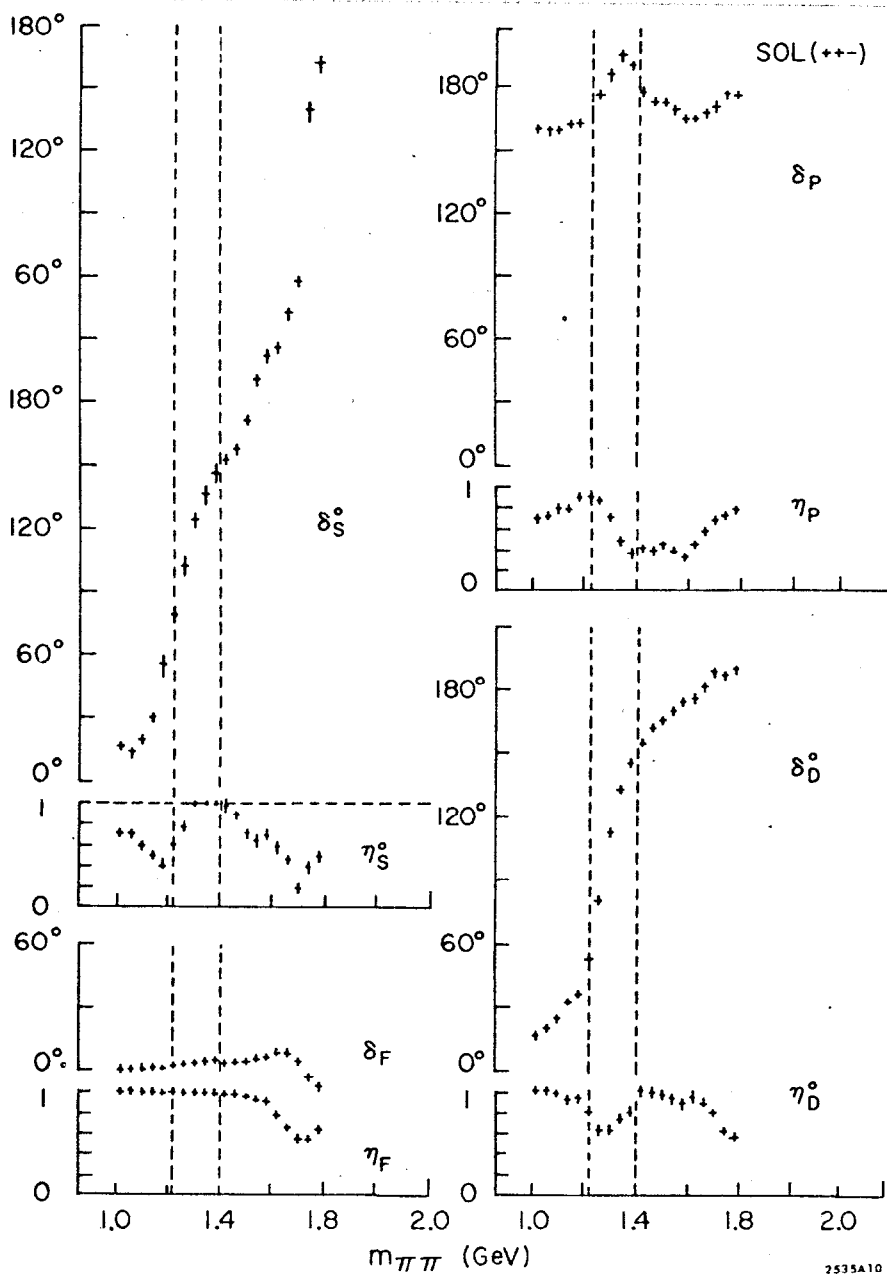


FIG. 22--Preliminary  $\pi\text{-}\pi$  phase shift — one of several possible solutions. See Ref. (15) for details.

Table VIII Daughter structure in natural parity mesons.

$J^{PG}, I$	$J^{PG}, I$
$\rho$ $1^{+-}, 1$	$\omega$ $1^{--}, 0$
$\epsilon$ $0^{++}, 0$	$\delta$ $0^{+-}, 1$
$A_2$ $2^{+-}, 1$	$f$ $2^{++}, 0$
$\circ$ $1^{--}, 0$	$\omega\pi$ $1^{-+}, 1$
$\circ$ $0^{+-}, 1$	$\epsilon'$ $0^{++}, 0$
$g$ $3^{-+}, 1$	$\omega'$ $3^{--}, 0$
$\circ$ $2^{++}, 0$	$\pi f$ $2^{+-}, 1$
$\rho'$ $1^{-+}, 1$	$\circ$ $1^{--}, 0$
$\circ$ $0^{++}, 0$	$\circ$ $0^{+-}, 1$

barrier, but, conversely, low lying states with a given  $J$  and  $k$  will imply a value of  $R$  much smaller than 1 fermi and should be suppressed due to their non-peripherality. Perhaps the small coupling of the  $\rho'$  to  $\pi\pi$  is a sign of such a suppression. Study of these low lying states will certainly be important in our full understanding of the properties in angular momentum space, of the non-diffractive  $\pi\pi$  elastic scattering amplitude. At any rate, as we push forward with studies of these low lying states — and it seems interesting to do so — we are again forced to consider seriously, the inelastic channels.

### EXOTICS

Cohen<sup>43</sup> has reviewed the status of experiments searching for exotic mesons at this meeting. The sensitivity of current experiments is  $\sim 50$ - $100$  events/ $\mu\text{b}$ . Since the existence of non  $q\bar{q}$  meson states is such a stringent test of the quark model

theories, it is important to push the limit on the existence of exotics as far as possible. The new multiparticle spectrometers — MPS, OMEGA, LASS offer a major increase in sensitivity, making  $10^3$ - $10^4$  event/ $\mu\text{b}$  experiments quite accessible. These experiments should be done.

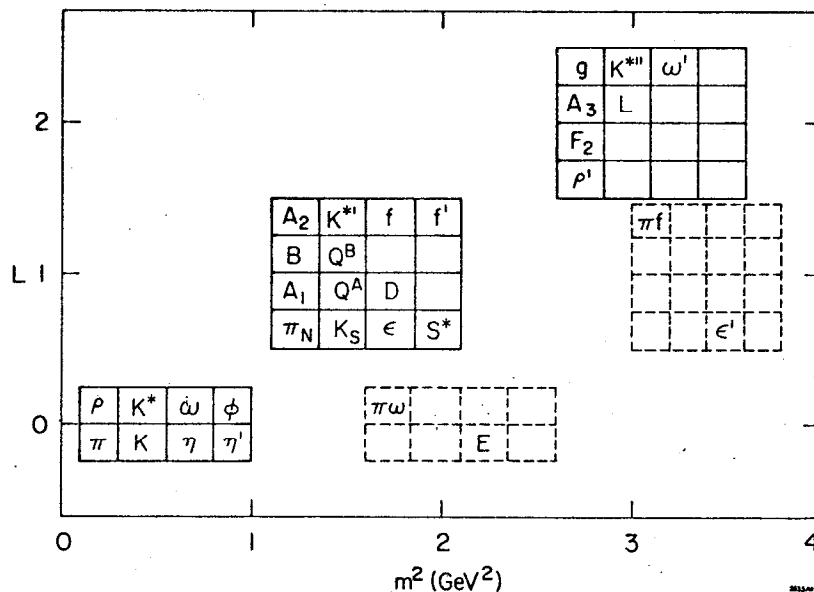


FIG. 23--Radial excitations of  $L=0$  and  $L$  quark model supermultiplets.

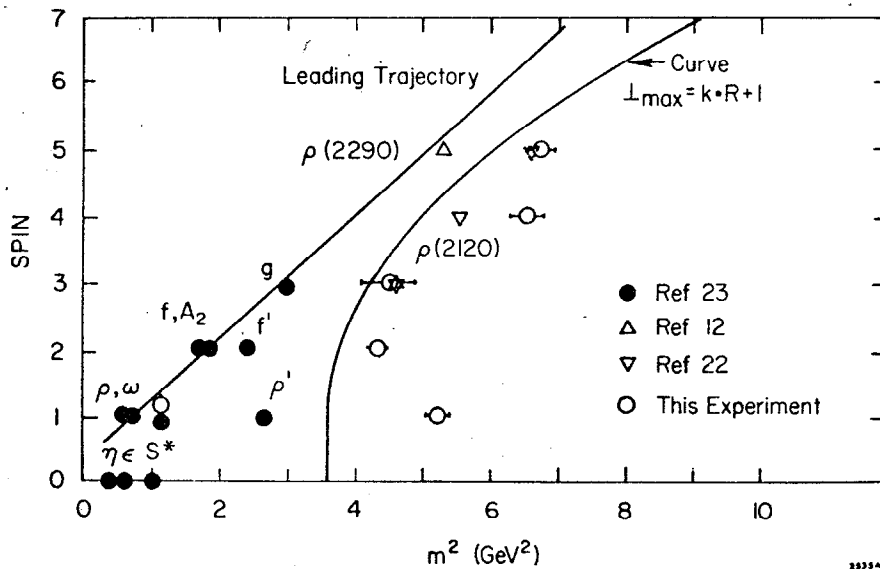


FIG. 24--Chew-Frautschi plot showing possible low lying  $\bar{N}\bar{N}$  states. See text and Ref. (42) for details.

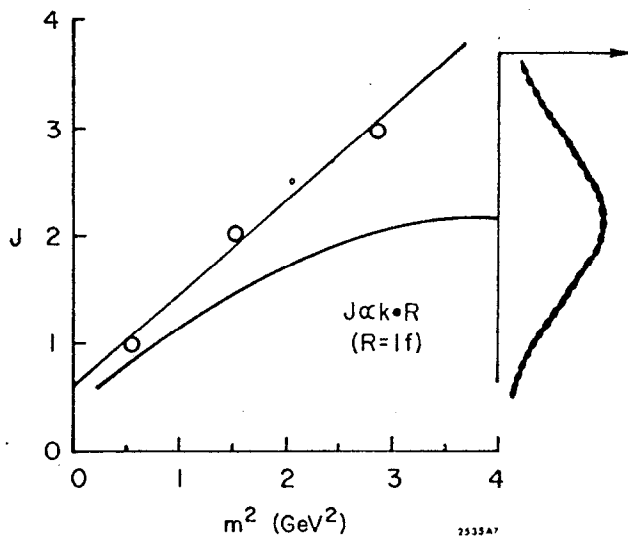


FIG. 25--Chew-Frautschi plot, showing the curve  $J \propto k \cdot R$ , with  $R = 1$  fermi. In addition to angular momentum barrier suppression of leading particles coupling to the  $\pi$ - $\pi$  channel, one should also expect this coupling of the low lying states to be suppressed due to their "non-peripherality."

#### HIGH ENERGY FOR DEMOCRACY

Finally I would like to comment on the possible use of very high energy beams to study meson spectroscopy. In all the reactions we have discussed so far, mesons are produced in  $t$ -channel exchange processes and so the ones we see are those that couple to healthy exchange amplitudes. This leads to the strong hierarchy we know in the meson world.

Perhaps, large  $P_T$  collisions are a way of producing mesons more democratically.

Let me make two observations on this: (a) we know that the cross section for exclusive processes becomes roughly equal at large momentum transfer. In Fig. 26, the differential cross section for several exclusive reactions involving pomeron,  $\pi$ ,  $K$ ,  $K^*$  and  $A_2$  exchange, are shown for beam

momenta of 4.0 and 5.0 GeV/c.<sup>44</sup> This is an indication of a rather democratic production mechanism dominating the large  $t$  region. (b) Let us suppose that the constituent interchange model<sup>45</sup> is a good guide to what is going

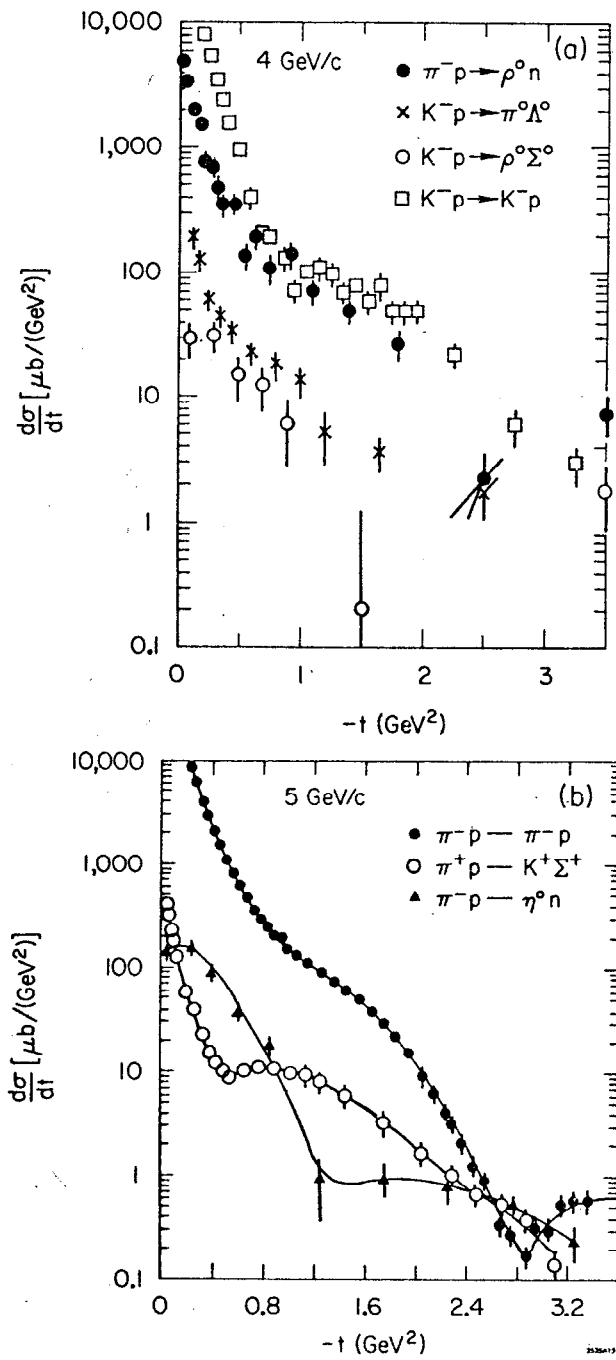


FIG. 26--The differential cross section for several exclusive channels at (a) 40 GeV/c, (b) 5.0 GeV/c, showing the near equality of all the reactions at large  $t$ .

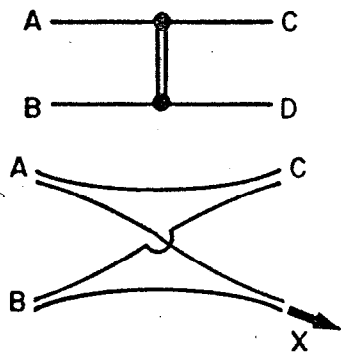


FIG. 27--Schematic diagrams for resonance formation in (a) peripheral collisions, (b) large  $P_T$  collisions.

on at large  $P_T$ . Then meson production may be thought to proceed as in Fig. 27. For small momentum transfers the exchange is dominated by some Regge-like mechanism, while for large  $P_T$  the reaction proceeds with the interchange of some fundamental constituent — say, the quarks. The meson final state "C" is produced when the quark and anti-quark come together to form mesonic matter. This  $q\bar{q}$  state may now project itself onto all the available meson states, and these states will have an equal probability of being formed, up to a statistical factor  $(2L + 1)$ , where  $L$  is the  $q\bar{q}$  relative angular momentum. We then have a situation where we may produce all mesons —  $\rho$ 's and  $\delta$ 's,  $A_2$ 's and  $D$ 's — with equal probability — an interesting and intriguing possibility.

Such experiments should become possible in the near future at NAL.

#### CONCLUSIONS

The following points serve to summarize this talk:

- It is important to have data on the meson states and their couplings to test the models of constituent interactions and resonance classification;
- from baryons we have learned that this requires systematic high statistics work on amplitude analysis for elastic and inelastic reactions;
- new tools are becoming available to help in these tasks
  - high data rate spectrometers with good multiparticle acceptance,
  - highly tuned partial wave analysis programs,
  - new capability with photon beams,
  - $e^+e^-$  facilities with high luminosity and  $4\pi$  magnetic detectors,
- maybe high energy and large  $P_T$  will provide a new view of the meson world.

#### ACKNOWLEDGMENTS

I would like to thank my colleagues at SLAC for many helpful discussions on the subject of this review. Special thanks go to R. K. Carnegie, M. Davier, F. Gilman and R. Schwitters.

## REFERENCES

1. S. Almeded and C. Lovelace Nucl. Phys. B40, 157 (1972).
2. R. Ayed and P. Baregre, Paper presented to the II<sup>nd</sup> Aix-en-Provence International Conference on Elementary Particles (1973).
3. R.D. Tripp, Paper presented at Berkeley APS Meeting on Particle Physics, p. 188, Berkeley, August 1973.
4. F.J. Gilman, Stanford Linear Accelerator Center Report No. SLAC-PUB-1320, Lectures presented at the Scottish University Summer School, 1973; and Invited talk at IV<sup>th</sup> International Conference of Experimental Meson Spectrometry, Boston, April 1974.
5. A.D. Brody et al., Phys. Letters 34B, 665 (1971); V. Mehtani et al., Phys. Rev. Letters 29, 1634 (1972); A. Kernan et al., Proceedings of Baryon Resonance Conference, p. 113, Purdue, 1973.
6. D.J. Herndon et al., Stanford Linear Accelerator Center Report No. SLAC-PUB-1108 (Rev.) and LBL 1065 (Rev.) submitted to Phys. Rev. (1974). A.H. Rosenfeld et al., Stanford Linear Accelerator Center Report No. SLAC-PUB-1386 and LBL 2633, submitted to Phys. Rev. Letters (1974). R.J. Cashmore et al., Stanford Linear Accelerator Center Report No. SLAC-PUB-1387 and LBL 2634, submitted to Phys. Rev. Letters (1974).
7. R.S. Longacre et al., Stanford Linear Accelerator Center Report No. SLAC-PUB-1390 and LBL 2637, submitted to Phys. Rev. Letters (1974). R.S. Longacre et al., Stanford Linear Accelerator Center Report No. SLAC-PUB-1389 and LBL 2636, to be submitted to Phys. Rev. R.S. Longacre (Ph. D. thesis) LBL-948 (1973).
8. D.J. Herndon, P. Soding and R.J. Cashmore LBL 543 (1973), submitted to Phys. Rev.
9. The notation used to describe our partial wave amplitudes is described fully in Ref. (6). The four character description gives the incident relative angular momentum, the outgoing relative angular momentum,  $2 \times$  the I-spin of the channel and  $2 \times$  the total spin, ( $L_{inc}$ ,  $L_{out}$ ,  $2I$ ,  $2J$ ). In addition there is an indication of the sub-particle state being considered  $\pi\Delta$ ,  $\rho N$ ,  $\epsilon N$ : since the spins of the  $\rho$ -meson and the nucleus may be combined to form total spin  $1/2$  or  $3/2$  there are two amplitudes denoted  $\rho_1 N$  or  $\rho_3 N$  respectively.
10. The Argand plots have been made using the "Baryon First" convention. A more detailed discussion is given in Ref. (6).
11. J. Rosner, Invited talk at the Berkeley APS Meeting on Particle Physics, p. 130, Berkeley, 1973 and Stanford Linear Accelerator Center Report No. SLAC-PUB-1391, submitted to Physics Reports.
12. F.J. Gilman, M. Kugler, S. Meshkov, Phys. Letters 45B, 481 (1973) and Stanford Linear Accelerator Center Report No. SLAC-PUB-1286, submitted to Phys. Rev. D. Faiman and J. Rosner, Phys. Letters 45B, 357 (1973).
13. D. Bowen et al., III<sup>rd</sup> International Conference on Experimental Meson Spectroscopy, p. 215 (1972), and Phys. Rev. Letters 29, 890 (1972).
14. R. Huff and J. Kirz, LRL Physics Note 474 (unpublished).
15. W. Manner, talk in these proceedings.
16. A. Barbaro-Galtieri et al., Meeting on  $\pi$ - $\pi$  Scattering, p. 1 (Florida 1973).

17. Aachen-Berlin-CERN-London-Vienna Collaboration. Paper submitted to Symposium on Multiparticle Dynamics, Leipzig, 1974.
18. G. Brandenburg, R.K. Carnegie, R.J. Cashmore, M. Davier, D.W.G.S. Leith, J.A.J. Matthews, P. Walden, S. Williams, F. Winkelman (private communication).
19. G. Ascoli, talk in these proceedings. Yu. M. Antipov et al., Contribution to IIIrd International Conference on Meson Spectroscopy, p. 164, 1972. G. Ascoli et al., Contributed paper to the 16th International Conference on High Energy Physics, Batavia, 1972.
20. T. Lasinski, talk in these proceedings.
21. T. Lasinski, et al., private communication.
22. R.K. Carnegie et al., private communication.
23. California Institute of Technology-LBL-SLAC Collaboration, private communication.
24. D.S. Ayres et al., Argonne Report ANL-HEP-7410, submitted to Phys. Rev. Letters.
25. L. Jones, talk in these proceedings.
26. Aachen-Berlin-CERN-London-Vienna Collaboration, CERN Reports — CERN/D. Ph II/74-1 and 74-10.
27. CERN-Munich Spectrometer — CERN, G. Grayer et al., Lindebaum-Ozaki Spectrometer — BNL  
K.J. Foley et al., Nucl. Inst. and Meth. 108, 33 (1973).  
Effective Mass Spectrometer — ANL.  
D.S. Ayres, Argonne Report ANL/HEP 7314.  
SLAC Spark Chamber Spectrometer — SLAC  
R.K. Carnegie et al., (private communication)
28. G. Luste and D.W.G.S. Leith, IInd International Conference on Experimental Meson Spectroscopy, p. 593 (1970).
29. K.W. Barnham et al., Nucl. Phys. B25, 49 (1970).
30. A. Michelini, invited talk presented at the International Conference on Instrumentation for High Energy Physics, Frascati, 1973.
31. Photon beam literature:  
Annihilation beams:  
J. Ballam et al., Nucl. Inst. and Meth. 73, 53 (1968).  
Coherent Diamond beams:  
G. Dianibrini Palazzi, Rev. Mod. Phys. 40, 611 (1968).  
Ash et al., Contribution to the Bonn Conference on Electron-Photon Physics, 1973.  
Polarized Bremsstrahlung by attenuation:  
N. Cabibbo et al., Phys. Rev. Letters 9, 270 (1962)  
Eisele et al., Nuc. Inst. and Meth. 113, 489 (1973).  
Back-scattered laser beam:  
R. Milburn, Phys. Rev. Letters 10, 75 (1963).  
C.K. Sinclair et al., IEEE Trans Nucl. Sci., 16, 1065 (1969).  
Tagged photon beams:  
G.R. Brookes et al., Nucl. Inst. and Meth. 85, 125 (1970).  
D. Caldwell et al., Phys. Rev. D7, 1362 (1973).
32. J. Rosen, talk in these proceedings.
33. K. Moffeit et al., Stanford Linear Accelerator Center Report No. SLAC-PUB-1004, submitted to Phys. Rev. M. Davier et al., Stanford Linear Accelerator Center Report No. SLAC-PUB-1205.

- 
34. F. Gilman and I. Karliner, Stanford Linear Accelerator Center Report No. SLAC-PUB-1382 (1974).
  35. T. Armstrong *et al.*, CERN Report CERN/SPSC/74-29.
  36. F. Martin, IIIrd International Conference on Meson Spectroscopy, p. 429 (1972).
  37.  $\rho'$  (1650):
    - G. Barbarino *et al.*, Lettere al Nuovo Cimento, 3, 689 (1972)
    - M. Grille *et al.*, Nuovo Cimento, 13 A, 593 (1973).
    - F. Ceradini *et al.*, Phys. Letters 43B, 341 (1973). $\rho'$  (1250):
    - M. Conversi *et al.*, Paper presented at this meeting.
  38. J. Rosner, Review of Resonances, Stanford Linear Accelerator Center Report No. SLAC-PUB-1391, submitted to Physics Reports (1974).
  39. W. Chinowsky, talk in these proceedings.
  40. Particle Data Group Tables, T. Lasinski *et al.*, submitted to Rev. Mod. Phys. (1974).
  41. J. Ballam *et al.*, Stanford Linear Accelerator Center Report No., SLAC-PUB-1373, submitted to Phys. Rev. (1974).
  42. B. Hyams *et al.*, CERN Report, submitted to Nucl. Phys. (1974).
  43. K. Cohen, talk in these proceedings.
  44. J.A.J. Matthews, talk presented at Berkeley APS Meeting on Particle Physics, Berkeley, 1973.
  45. R. Blankenbecler, S. Brodsky and R. Gunion, Phys. Letters 39B, 649 (1972); Phys. Rev. D6, 2652 (1972).